

Aus der Augenklinik und Poliklinik der Ludwig-Maximilians-  
Universität München

Direktor: Prof. Dr. Anselm Kampik

**Ultrastructural Analysis of Internal Limiting Membrane  
Removed during Vitrectomy with  
and without Dye Assistance**

Dissertation  
zum Erwerb des Doktorgrades der Medizin  
an der Medizinischen Fakultät der  
Ludwig-Maximilians-Universität zu München

vorgelegt von  
Yang Yang

aus  
Hubei, China

Jahr  
2011

Mit Genehmigung der Medizinischen Fakultät  
der Universität München

Berichterstatter: Prof. Dr. Arnd Gandorfer

Mitberichterstatter: Prof. Dr. Josef Müller-Höcker

Mitbetreuung durch den  
promovierten Mitarbeiter: Dr. Ricarda Schumann

Dekan: Prof. Dr. med. Dr. h.c. M. Reiser, FACR, FRCR

Tag der mündlichen Prüfung: 17.03.2011

# CONTENTS

Abstracts .....	1
i. Zusammenfassung .....	1
ii. Summary .....	3
1 INTRODUCTION.....	5
1.1 Normal Anatomy.....	5
1.1.1 The vitreoretinal interface .....	6
1.1.1.1 Outer vitreous cortex fibrils.....	6
1.1.1.2 Internal limiting membrane.....	6
1.1.1.3 The processes of Müller cells .....	7
1.1.2 Morphological characteristics of cells implicated in the pathogenesis of traction maculopathien .....	8
1.1.2.1 Müller cell.....	8
1.1.2.2 Fibrous Astrocyte.....	8
1.1.2.3 Myofibroblast .....	9
1.1.2.4 Fibroblast.....	9
1.1.2.5 Macrophage.....	9
1.1.2.6 Retinal pigment epithelial cell .....	10
1.1.2.7 Hyalocyte .....	10
1.2 Pathogenesis of vitreoretinal diseases .....	10
1.2.1 Macular holes.....	11
1.2.2 Macular pucker .....	12
1.2.3 Vitreomacular traction syndrome .....	12
1.2.4 Diabetic retinopathy .....	12
1.2.5 Proliferative vitreoretinopathy.....	13
1.3 Surgical treatment .....	13
1.3.1 Pars plana vitrectomy.....	13
1.3.2 Staining of the ILM .....	14
1.3.2.1 Different dyes .....	14
1.3.2.1.1 Indocyanine green.....	14
1.3.2.1.2 Trypan blue and membrane blue .....	14
1.3.2.1.3 Brilliant blue .....	14
2 MATERIALS AND METHODS .....	16
2.1 Laboratory Equipment.....	16
2.2 Reagents .....	18
2.3 Prescription.....	18
2.4 Materials.....	20
2.5 Methods.....	21
2.5.1 Preparation.....	22
2.5.1.1 Fixation .....	22
2.5.1.2 Washing .....	22
2.5.1.3 Postfixation.....	23

2.5.1.4	Washing .....	23
2.5.1.5	Dehydration .....	23
2.5.1.6	Transitional solvent.....	23
2.5.1.7	Embedding.....	23
2.5.2	Microtomy and Light microscopy.....	24
2.5.3	Electron microscopy.....	24
2.5.4	Statistical Analysis .....	25
3	RESULTS.....	26
3.1	Clinical features.....	26
3.2	Morphological features .....	27
3.2.1	Light microscopic features .....	27
3.2.1.1	Vitreous side of the ILM .....	27
3.2.1.2	Retinal side of the ILM.....	28
3.2.1.3	Single cells crossing the ILM.....	28
3.2.2	Electron microscopic features.....	29
3.2.2.1	ILM in electron microscopy .....	29
3.2.2.2	Four distinct morphologic patterns of retinal structures .....	29
3.2.2.3	Pattern of cellular elements depending on the disease in the group without dye administration .....	29
3.2.3	Comparison between different groups .....	30
3.2.3.1	Cell proliferation .....	30
3.2.3.2	Dye administration .....	30
3.2.3.3	Diseases.....	30
	Figures and tables.....	32
4	DISCUSSION .....	50
4.1	Principal findings .....	50
4.1.1	Morphologic changes on both sides of the ILM.....	50
4.1.2	Explaining of the results.....	51
4.2	Strengths and weaknesses of the study .....	51
4.3	Strengths and weaknesses in relation to other studies.....	52
4.4	Meaning of the study.....	53
4.5	Unanswered questions and future research .....	54
	References .....	55
	Acknowledgements .....	59
	Curriculum Vitae.....	60

## Abstracts

### i. Zusammenfassung

Die Entfernung der inneren Grenzmembran (internal limiting membrane, ILM) der Netzhaut während der Vitrektomie hat sich weitgehend als effektive Therapieoption in der Makulaforamenchirurgie für bestmögliche funktionelle und anatomische Ergebnisse durchgesetzt. Der ILM kommt bei der Untersuchung der vitreoretinalen Grenzfläche eine zentrale Bedeutung zu, da sie chirurgisch gewonnen und untersucht werden kann, wie vitreale und epiretinale Traktionen auf die Netzhaut übertragen werden. Im Gegensatz zu den morphologischen Veränderungen der vitrealen Seite der ILM, sind die Kenntnisse über morphologische Veränderungen der retinalen Seite der ILM auf wenige Untersuchungen beschränkt.

Ziel dieser Untersuchung war, das Vorkommen retinaler Zellen und Zellreste an der inneren Grenzmembran bei 109 Patienten zu untersuchen.

Es wurde bei 79 Augen mit Makulaforamina (MF) und bei 30 Augen mit anderen traktiven Makulopathien eine Vitrektomie durchgeführt. Die Patienten wurden in zwei Gruppen eingeteilt: eine Gruppe ohne Anwendung intravitrealer Farbstoffe und eine zweite Gruppe mit Anwendung intravitrealer Farbstoffe. Die Gruppe ohne Anwendung intravitrealer Farbstoffe bestand aus 32 idiopathischen MF, 13 rezidivierenden MF, 8 sekundären MF, 11 Makular Pucker, 1 Augen mit Diabetischer Retinopathie, 3 Augen mit Proliferativer Vitreoretinopathie, und 6 Augen mit Vitreomakulärem Traktionssyndrom. Die Gruppe mit Anwendung intravitrealer Farbstoffe bestand aus 17 idiopathischen MF, 6 rezidivierenden MF, 3 sekundären MF, 6 Makular Pucker und 3 Augen mit Diabetischer Retinopathie.

Alle Präparate wurden nach der Entfernung bei der Operation sofort in 4% Glutaraldehyd fixiert und mit Osmiumtetroxid nachfixiert. Die Präparate wurden für die konventionelle Licht- und Elektronenmikroskopie in Serienschnitten aufbereitet. 1379 Semidünnschnitte und über 400 Ultradünnschnitte wurden ausgewertet.

Im lichtmikroskopischen Bild zeigte sich die ILM als dünnes blaues Band in allen Präparaten. Von den 109 Patienten fanden sich bei 41 Patienten vitreale Zellen oder Zellreste in der Gruppe ohne Anwendung intravitrealer Farbstoffe und bei 20 Patienten in der Gruppe mit Anwendung intravitrealer Farbstoffe. Retinale Zellen oder Zellreste fanden sich bei 16 Patienten in der Gruppe ohne Anwendung intravitrealer Farbstoffe und bei 9 Patienten in der Gruppe mit Anwendung intravitrealer Farbstoffe.

Beim Vergleich idiopathischer Makulaforamina und Macular pucker mit und ohne Farbstoff wurden signifikant wenige retinale Zellreste gefunden in der Gruppe ohne Anwendung intravitrealer Farbstoffe. Verglichen mit anderen Makulopathien wurden signifikant weniger Zellreste bei Makulaforamina gefunden in der Gruppe ohne Anwendung intravitrealer Farbstoffe. 15,1% aller Makulaforamina und 38,1% der anderen Makulopathien hatten Zellreste an der retinalen Seite der ILM. Es zeigte sich kein Unterschied in Abhängigkeit von Alter, Auge oder Operateur.

Bei den 25 Patienten, bei denen lichtmikroskopisch retinale Zellreste gefunden wurden,

wurde eine elektronenmikroskopische Untersuchung durchgeführt, um die gleiche Stelle zu treffen, an der Zellreste im lichtmikroskopischen Bild gefunden wurden. Die retinalen Zellreste wurden anhand des elektronenmikroskopischen Bildes der Grösse und der Form nach in vier Grade eingeteilt. Grad 1 entspricht kleinen runden Zellfragmenten, deren Durchmesser weniger als 1  $\mu\text{m}$  war. Grad 2 entspricht mittleren runden Zellfragmenten, deren Durchmesser zwischen 1 und 2  $\mu\text{m}$  war. Grad 3 entspricht großen irregulären Zellfragmenten, deren Durchmesser größer als 2  $\mu\text{m}$  war. Grad 4 entspricht vollständigen Zellen mit Zellorganellen wie Zellkern, Mitochondrien, Golgi-Komplex und Endoplasmatischem Retikulum. Von den 8 Makulaforamen-Patienten mit retinalen Zellfragmenten in der Gruppe ohne Anwendung intravitrealer Farbstoffe zeigte kein Patient ganze Zellen (Grad 4), während bei den anderen Traktionsmakulopathien in der Gruppe ohne Anwendung intravitrealer Farbstoffe 63% der Präparate ganze Zellen an der retinalen Seite der ILM zeigten. Dieser Unterschied könnte durch die stärkere Traktion und Fältelung der ILM bei diesen Erkrankungen mitbedingt sein.

## ii. Summary

Removal of the internal limiting membrane (ILM) during vitrectomy is widely accepted as an effective therapy for macular holes and other traction maculopathies. The ILM plays an important role in these diseases, because it can transmit vitreal and epiretinal traction to the retina. Compared to the morphological changes on the vitreal side of the ILM, the understanding of the retinal side is limited.

The purpose of this study was to investigate the cells and cell fragments on the retinal side of the ILM in 109 patients.

Vitrectomy was performed in 79 eyes with macular holes and 30 eyes with other traction maculopathies. The patients were divided into two groups: without vital dye and with vital dye administration. We included 32 eyes with idiopathic macular holes, 13 eyes with recurrent macular holes, 8 eyes with secondary macular holes, 11 eyes with macular pucker, one eye with diffuse macular edema in proliferative diabetic retinopathy, 3 eyes with proliferative vitreoretinopathy and 6 eyes with vitreomacular traction syndrome in the group without dye administration. In the dye administration group, we included 17 eyes with idiopathic macular holes, 6 eyes with recurrent macular holes, 3 eyes with secondary macular holes, 6 eyes with macular pucker and 3 eyes with proliferative diabetic retinopathy. All specimens were immediately placed in 4% glutaraldehyde for fixation after removal during surgery. Osmium tetroxide was used for postfixation. The specimens were prepared for conventional light and electron microscopy in serial sections. 1379 light- and more than 400 electronmicroscopic sections were evaluated.

In light microscopy, the ILM showed a thin strand in all specimens. Cells and cell fragments were found in 41 specimens in the group without dye administration and in 20 specimens in the group of dye administration on the vitreal side of the ILM. On the retinal side of the ILM, cell fragments were found in 16 specimens at the ILM by light microscopy in the group without dye administration and in 9 specimens in the dye administration group.

A significant difference was seen between the presence of retinal debris between the group without dye administration and the dye administration group, when comparing idiopathic macular hole and macular pucker eyes only. Significant fewer cells or cell fragments were observed in macular holes in the group without dye administration, compared with other traction maculopathies. About 15.1% of specimens with macular holes and 38.1% with other traction maculopathies showed cell fragments on the retinal side of the ILM. No difference was shown depending on age, eye, or surgeon.

Twenty-five specimens in whom retinal cell fragments were found were evaluated by electron microscopy. Four distinct morphologic patterns were observed on the retinal side of the ILM depending on the size and shape of cellular fragments. Grade 1 were small round cell fragments <1  $\mu\text{m}$  in diameter. Grade 2 were medium sized (1-2  $\mu\text{m}$  in diameter) cell fragments. Grade 3 were large cell fragments of more than 2  $\mu\text{m}$  in diameter. Grade 4 were entire retinal cell bodies with cellular organelles such as nucleus, mitochondriae, golgi complexes, and endoplasmatic reticulum. In the group without dye administration, complete retinal cell bodies were not seen in eyes with macular holes, but in 63% of eyes with other traction maculopathies. The difference could be caused by more severe traction and

puckering of the ILM in other traction maculopathies compared with macular hole eyes.



# 1 INTRODUCTION

Peeling of the internal limiting membrane (ILM) during macular surgery is a procedure widely accepted in macular traction disorders. The rationale for peeling the ILM is to relieve vitreoretinal traction. Tangential or antero-posterior traction to the retina exerted by the vitreous or epiretinal membranes (ERM) may promote glial cell migration and proliferation. Numerous studies show that removal of the ILM during macular surgery has a favorable functional and anatomical outcome and minimizes the recurrence of ERM. (Park, Sipperley et al. 1999; Brooks 2000; Gandorfer, Messmer et al. 2000; Mester and Kuhn 2000; Smiddy, Feuer et al. 2001; Scott, Moraczewski et al. 2003; Al-Abdulla, Thompson et al. 2004; Kwok, Lai et al. 2005; Haritoglou, Schumann et al. 2006; Patel, Hykin et al. 2006) However, there are some reports demonstrating functional deficits mostly after dye-assisted ILM removal. (Haritoglou, Gass et al. 2001; Gass, Haritoglou et al. 2003; Haritoglou, Gandorfer et al. 2003) This made researchers paying more attention to a potential retinal injury caused by the ILM-peeling itself or by the vital dye used for better visualization of the translucent ILM.

The ILM is the basal lamina of Müller cells. Their footplates are directly adjacent to the ILM. Any injury of these footplates or of Müller cell bodies may affect retinal neurons because Müller cells hold a number of functions in the retinal cell structure. (Newman and Reichenbach 1996) They are thought to be important for neuronal waste exchange. Müller cells supply endproducts of anaerobic metabolism for neurons and synthesize retinoic acid from retinol. They are involved in phagocytosis of neuronal debris and release neuroactive substances. Thus, removal of the ILM with potential damage to Müller cells may influence functional outcome.

The retinal injury may leave cells or cell fragments on the retinal side of the ILM. After indocyanine green (ICG)-assisted ILM removal, ultrastructural and histopathologic studies reported on the presence of retinal cell fragments at the ILM derived from Müller cells. (Gandorfer, Haritoglou et al. 2001; Haritoglou, Gandorfer et al. 2002) In previous studies on ILM removal without intravitreal dye administration, these retinal cell fragments appeared rather small or were not found at all. (Schumann, Schaumberger et al. 2006; Schumann, Gandorfer et al. 2009) However, an investigation of a large series of ILM specimens removed without staining is still pending. Therefore, we focused on the retinal side of the ILM and evaluated 109 surgical ILM specimens obtained during macular surgery with and without intravitreal dye administration.

## 1.1 Normal Anatomy

The vitreoretinal interface is defined as the structure situated between the outer vitreous cortex and the plasma membrane of the Müller cell. It is the site of five potentially blinding vitreoretinal disorders: macular hole, macular pucker, diabetic vitreoretinopathy, proliferative vitreoretinopathy and vitreomacular traction syndrome. (Sebag and Hageman 2000)

### 1.1.1 The vitreoretinal interface

The vitreoretinal interface consists of three components, which are: anchoring fibrils of the vitreous body, the internal limiting membrane and the cell membrane of Müller cells adjacent to the retinal side of the ILM.

There are attachments to the internal limiting membrane from both the retina and the vitreous. On the retinal side, the terminal extensions of the Müller cells form an uneven but continuous border. By varying its thickness, the ILM fills in areas of relative excavation in the uneven surface of the Müller cell endfeet, producing a smooth inner surface of the retina.

#### 1.1.1.1 Outer vitreous cortex fibrils

The vitreous is composed of 97%-99% water and the remaining tissue includes mainly collagen fibrils, glycosaminoglycan, hyaluronan and chondroitin sulfate. (Scott 1992) The collagen fibrils are thought to be charged of the connection between the vitreous gel and the internal limiting membrane. There are no direct connections between the posterior vitreous cortex and the retina. Only at the retinal periphery fibers of the vitreous body can be seen passing into the internal limiting membrane. The exact nature of the adhesion between the posterior vitreous cortex and the ILM is not known, but most probably results from the action of the various extracellular matrix molecules found at this interface, including fibronectin and laminin. (Sebag 1991; Sebag 1992)

#### 1.1.1.2 Internal limiting membrane

Three horizontal membranes have been identified within the retina, but only one of these, the internal limiting membrane, has the characteristic structure of a basement membrane. Although the middle limiting membrane and the external limiting membrane has both the light microscopic appearance of membranes and a potential metabolic barrier function, neither of them is a true basement membrane. The middle limiting membrane is a pseudomembrane formed by the photoreceptor and bipolar cell synapse, which are juxtaposed in the inner zone of the outer plexiform layer. The external limiting membrane is formed by the continuous line of intermediate junctions between adjacent photoreceptor cells and the Müller cells.

The inner limiting membrane is seen as delicate collagen-like fibrils in a dense matrix. It is separated from the Müller cells by an electron-lucent zone which is traversed by fibrils. (Foos 1972) At the posterior pole, the membrane is 10-20  $\mu\text{m}$  thick and shows an irregular outer surface which follows the contours of the Müller cells. It has a flat inner surface, with delicate collagen-like fibrils of the vitreous cortex. (Fine and Tousimis 1961)

Ultrastructural work has shown that it consists of a true basement membrane, with

intimate association with the collagen fibrils of the vitreous body and with the cell membrane of Müller cells.

In electron microscopy, the internal limiting membrane is composed of three structures as other basement membranes: lamina fibroreticularis, lamina densa and lamina lucida. Ultrastructural studies have shown that the inner portion of the internal limiting membrane, the lamina fibroreticularis, is formed by vitreous fibrils; the middle portion, lamina densa, is formed by collagen, and the outer portion, lamina lucida, consists mostly of the basement membrane of Müller cells. (Foos 1972)

The internal limiting membrane is also termed basal lamina of the retina, internal limiting lamina or Membrana limitans interna retinae in the literatures. It has been studied since 1871. (Heegaard 1997)

A regional difference in thickness of the ILM was found in human adult eyes. The ILM is thickest in the macular region. The length of vitreous fibrils close to the ILM also varied between the four regions in human eyes. The longest fibrils are in the ora serrata region, the second longest in the equatorial region, the next longest in the optic disc region and the shortest in the macular region. (Heegaard 1997)

### 1.1.1.3 The processes of Müller cells

Müller cells are the largest cells in the retina and the predominant macroglial cell of the retina. These cells span the entire thickness of the retina and maintain the structure of the retina and are the only cell type that occupies the full thickness of the retina from the external to the internal limiting membrane. Their cytoplasmic extensions reach between and envelop neuronal cell bodies and processes, filling all intercellular spaces except for synapses between the neural cells, spaces in the adventitia of large blood vessels, and the small (less than 20 nm) potential spaces between ganglion cell axons and dendrites. This vast extension of Müller cell processes effectively enmeshes the remainder of the retina so that all cell bodies and cellular processes between the external and internal limiting membranes reside in tunnels formed by Müller cells.

The mature Müller cell has four types of cell processes. Radial processes arise from both sides of the cell body in the internal nuclear layer and extend through the retinal processes to form part of the internal limiting membrane. Fine horizontal processes extend laterally in the two plexiform layers and through the nerve fiber layer.

## 1.1.2 Morphological characteristics of cells implicated in the pathogenesis of traction maculopathien

### 1.1.2.1 Müller cell

In theory, disease of the Müller cells could reflect itself in both metabolic and structural changes in the retina because of its intimate association with all retinal cells and vasculature and with the space between the photoreceptor outer segments and pigment epithelium. Müller cells constitute an anatomical link between the retinal neurons and the compartments with which they need to exchange molecules, i. e., the retinal blood vessels, the vitreous body, and the subretinal space. This link is not merely anatomical but also functional. For this purpose, Müller cells are endowed with a wealth of different ion channels, ligand receptors, transmembraneous transporter molecules, and enzymes. Many of these molecules are not found in retinal neurons or other retinal cell types and are specifically expressed by Müller cells, or at least, are most abundant in Müller cells. (Newman and Reichenbach, 1996; Sarthy and Ripps, 2001)

### 1.1.2.2 Fibrous Astrocyte

Besides Müller cells, there is another macroglial cell, the astrocyte, in the retina. Astrocytes migrate into the retina via the optic nerve during embryogenesis and become located exclusively in the inner layers of the retina. Astrocytes are satellite in shape and their cell bodies are located in the ganglion cell layer. Their processes show no strict orientation. (Watanabe and Raff 1988)

Astrocytes are widely dispersed between the vasculature and neurons. Morphologic and cytoplasmic features of these cells allow them to be categorized into fibrous astrocytes and protoplasmic astrocyte. (Bussow 1980)

A fibrous astrocyte has a homogeneous cytoplasm with a dense round or oval nucleus, and a sparse endoplasmic reticulum. They contain a noticeable concentration of glycogen granules, elongated mitochondria, microtubules, a cilium, and an occasional centriole. (Kampik, Kenyon et al. 1981)

On electron microscopy these cells are characterized by masses of intracytoplasmatic intermediate type 8- to 10-nm filaments and junctional complexes of the adherence type.

Within the ganglion cell layer, the astrocytes tend to lie horizontally, surrounding the blood vessels. Their long, slender processes form interconnected honeycomblike scaffolding between vessels and neural cells. This network lies parallel to the interal limiting membrane and perpendicular to the Müller cells. The processes form an irregular pattern of interconnections with processes that reach over into the inner nuclear layer. There are no astrocytes centrifugal to the inner nuclear layer, so the outer plexiform and outer nuclear

layer has no astrocytes in the far peripheral retina or in the fovea. (Bussow 1980)

### 1.1.2.3 Myofibroblast

Myofibroblasts are well known as a cellular participant in wound-healing, a variety of inflammatory or fibrosing non-neoplastic conditions, and tumor growth. (Walshe, Esser et al. 1992; Eyden, Banerjee et al. 2009)

Myofibroblast share features with fibroblasts (rough endoplasmic reticulum, Golgi apparatus) and expression of smooth muscle actin. However they are devoid of lamina- $\alpha$  structure seen in smooth muscle cells. (Eyden, Banerjee et al. 2009)

Myofibroblasts are of a spindled or satellite morphology, immunostaining for  $\alpha$ -smooth muscle actin ( $\alpha$ -SMA). Ultrastructure features of myofibroblasts are fusiform nucleus and cell body, rough endoplasmic reticulum, aggregate of 5-7nm subplasmalemmal cytoplasmic filaments, and the absence of intracytoplasmic intermediate type 10 nm filaments or basement membran. (El-Labban and Lee 1983; Eyden, Banerjee et al. 2009)

### 1.1.2.4 Fibroblast

Fibroblasts are the main cells in the connective tissue. The cell synthesis collagen fibrils and often reside in close association with the collagen bundles. The cell has a dark stained, large and ovoid nucleus, and a well-defined nucleolus. Electron microscopy reveals a fusiform cell body and nucleus, abundant rough endoplasmic reticulum and a prominent golgi complex. (Krieg, Abraham et al. 2007)

### 1.1.2.5 Macrophage

Macrophages belong to the mononuclear phagocytic system. These cells are active phagocytes. Their functions are removing cellular debris and protecting the body against foreign invaders. (van Furth, Raeburn et al. 1979)

Macrophages measure about 10-30  $\mu$ m in diameter and are irregularly shaped. Active macrophages have pleats and folds in their plasma membrane as a consequence of cell movement and phagocytosis. Their cytoplasm contains many vacuoles and small dense granules. The nucleus is eccentric and usually has no nucleoli. Electron microscopy demonstrated an irregular shape of the nucleus, a well-developed Golgi apparatus, prominent rough endoplasmic reticulum, abundance of lysosomes, and multiple intracytoplasmic vesicles. (Ryter 1985)

### 1.1.2.6 Retinal pigment epithelial cell

The retinal pigment epithelium (RPE) cells are considered to be multifunctional pluripotent cells. The RPE has a polarization with a basement membrane. Each RPE cell is polarized with an apical part adjacent to the subretinal space and a basal portion facing Bruch's membrane. The cells are ultrastructurally characterized by intracytoplasmic melanin granules, microvilli and junctional complexes. They extend from the margin of the optic disc to the ora serrata, where they are continuous with the pigmented epithelium of the pars plana of the ciliary body. (Gotzinger, Pircher et al. 2008) RPE cells have various functions. The essential one is the charge of metabolism of photoreceptors. They are also related to vitamin A metabolism and regeneration in the visual cycle, phagocytosis and degradation of shed outer segment tips, light absorption by melanin granules, heat exchange, secretion of the matrix surrounding the photoreceptor inner and outer segments, and active transport of materials between the choriocapillaris and the subretinal space. (Strauss 2009)

### 1.1.2.7 Hyalocyte

Hyalocytes are distributed in the vitreous cortex in a single layer situated 20-50  $\mu\text{m}$  away from the internal limiting membrane at the posterior retina and the basal lamina of the ciliary epithelium at the pars plana and vitreous base. (Sebag 1992)

The ultrastructural features of hyalocytes have been described since the 1960s. These cells are oval or spindle-shaped, 10-15  $\mu\text{m}$  in diameter, and contain a lobulated nucleus, a well-developed Golgi complex, smooth and rough endoplasmic reticula, and many large PAS-positive lysosomal granules and phagosomes. (Bloom and Balazs 1965)

The main physiological functions of the hyalocytes are thought to be related to protein synthesis, e.g. hyaluronan synthesis, collagen synthesis, glycoprotein production and certain enzymes. (Sebag 1992)

## 1.2 Pathogenesis of vitreoretinal diseases

The intimate connection of the internal limiting membrane with the Müller cells suggests a common pathogenesis of the five vitreomacular interface diseases. The relationship of the internal limiting membrane to the cortical vitreous will produce a wrinkling of the retina if the membrane is affected by a cortical vitreous contraction. Besides the commonness, individual pathogenesis depends on the strength and the results of the traction force.

## 1.2.1 Macular holes

Idiopathic macular holes are characterized by a dehiscence of the neuroretina at the fovea, leading to loss of central vision, metamorphopsia, and a central scotoma. (la Cour and Friis 2002)

The majority of macular holes are primary idiopathic with a small proportion being a result of trauma, inflammation or high myopia. (McDonnell, Fine et al. 1982)

There were many theories on the pathogenesis of macular holes, such as anteroposterior vitreous traction bands (Lister 1924), age-related changes in the retinal vasculature leading to cystoid degeneration, responsible for atraumatic macular holes, vascular theory characterized as ocular angiospasm, and cystoid degeneration as the final common pathway towards macular hole formation.

In 1988, Gass proposed a classification system for idiopathic macular holes, as well as a new hypothesis concerning their pathogenesis, suggesting that tangential vitreoretinal traction is responsible for macular hole formation. (Gass 1988) In 1995, Gass provided an updated biomicroscopic classification and anatomic interpretation of macular hole formation: (Gass 1995)

Grade 1: The hole commences as a foveal intraretinal cyst (stage 1A) or ring of cysts (stage 1B) seen as a central yellow spot or ring of spots. The patient may be asymptomatic or have mild visual disturbances or image distortion.

Grade 2: A small crescentic or round hole of less than 400  $\mu\text{m}$  in diameter.

Grade 3: A large round hole of more than 400  $\mu\text{m}$  in diameter.

Grade 4: A hole with an associated posterior vitreous detachment (PVD).

(Gass 1988)

The development of macular holes begins with a yellow spot or ring in the center of the fovea, and the fovea loses its depression. In some cases, spontaneous separation of the vitreous without macular hole formation may occur, in other cases, a pseudo-operculum appears above the hole. When the yellow spot or ring expanded, the initial break often occurred eccentrically near one edge of the ring, and it enlarged in a can-opener fashion over a period of weeks or several months to form initially a crescent-shaped macular hole, followed by a horseshoe-shaped macular hole, and finally by a round macular hole with an operculum attached to the posterior hyaloid surface. (Gass 1988)

An ultrastructural study showed that fibrous astrocytes, myofibroblasts, fibroblasts, and macrophages were observed in descending order in ILM specimens obtained from patients with macular holes. Analysis of cellular distribution showed that mono- and multilayered cellular membranes were seen more frequently in stage IV macular holes than in stage III macular holes. The presence of native vitreous collagen was always associated with fibrocellular proliferation. (Schumann, Schaumberger et al. 2006)

### 1.2.2 Macular pucker

Macular pucker is a term used for premacular membranes which cause macular surface distortion or visual impairment by membrane contraction. The exact pathogenesis of macular pucker remains unknown. The migration and proliferation of glial cells may play a predominant role. (Smiddy, Maguire et al. 1989) An epiretinal membrane forming a macular pucker may have more than one site of retinal contraction. (Gupta, Sadun et al. 2008)

### 1.2.3 Vitreomacular traction syndrome

Vitreomacular traction syndrome is characterized by a persistent attachment of the vitreous to the macula in eyes with an incomplete posterior vitreous detachment. (Gandorfer, Rohleder et al. 2002) The most common morphological configuration is a vitreous separation peripheral to a zone where the cortical vitreous remains attached to the retina at the macula and the optic nerve head. Ultrastructural investigation revealed that myofibroblasts were the predominant cell type. (Gandorfer, Rohleder et al. 2002)

### 1.2.4 Diabetic retinopathy

Diabetic retinopathy is characterized clinically by hemorrhages, microaneurysms, cotton-wool spots, lipid exudates, macular edema, capillary occlusion, and neovascularization. Neovascularization is the criterium for subdividing the disease into a nonproliferative and a proliferative form. Recent research indicates that diabetic retinopathy includes not only a microvascular but also a neuronal component.

Müller cells have a direct effect in the formation of diabetic epiretinal membranes. Astrocytes were found undergoing severe changes in diabetics, such as the production of cytokines such as VEGF. (Barber, Antonetti et al. 2000) These cytokines can increase vessel permeability, (Cooper, Vranes et al. 1999) and act secondary on endothelial cells to reduce their ability to form tight junction. (Barber, Antonetti et al. 2000)

Ultrastructural features of epimacular membranes from patients with proliferative diabetic retinopathy showed that the membranes were mostly multilayered consisting of predominantly fibroblasts and fibrous astrocytes situated on a layer of native vitreous collagen. Macrophages were present in most specimens; retinal pigment epithelial cells were not found. (Gandorfer, Rohleder et al. 2005)



## 1.2.5 Proliferative vitreoretinopathy

Proliferative vitreoretinopathy (PVR) is characterized by the growth and contraction of cellular membranes within the vitreous cavity and on both retinal surfaces. It is not a specific clinical disease, but a consequence of a number of intraocular diseases with various stimuli such as retinal detachment and it is the major cause of failure of retinal detachment surgery. (Pastor, de la Rúa et al. 2002)

Lots of cells are implicated in the pathogenesis of PVR. Müller cells in fibroproliferative membranes may transdifferentiate into myofibroblasts that generate tractional forces in response to growth factors in the vitreous, thereby causing traction retinal detachment. (Guidry 2005)

Ultrastructural features of epiretinal membranes from patients with PVR showed that cell proliferation could be found in each specimen, and fibrous astrocytes, fibrocytes, macrophages and myofibroblast were the predominant cell types. (Kampik, Kenyon et al. 1981)

## 1.3 Surgical treatment

### 1.3.1 Pars plana vitrectomy

Pars plana vitrectomy (PPV) is the most versatile surgical techniques to treat vitreoretinal disorders. It was performed by Machemer for the first time in the early 1970s. Later Machemer improved this technique with an intraocular fiberoptic light pipe and separated the probes for various functions.

Kelly and Wendel introduced vitrectomy to close macular holes in 1991. The surgical technique consists of a pars plana vitrectomy and removal of the posterior hyaloid. Epiretinal membranes if present should be removed. The removal of ILM is also recommended to enhance the closure rate and functional outcome. A fluid-air exchange and an air-gas exchange follow. Face-down positioning is required for at least 4 days. (Kelly and Wendel 1991)

Some studies demonstrated a good outcome after vitrectomy with ILM-peeling in macular pucker eyes. (Park, Dugel et al. 2003; Kwok, Lai et al. 2005) In case of short duration the surgical treatment can obtain the best results.

The vitreous hemorrhage caused by proliferative diabetic retinopathy is one of the most common indications for vitrectomy. Vitrectomy releases posterior vitreous traction which reduces the stimulus for retinal neovascularization.

## 1.3.2 Staining of the ILM

The ILM is a translucent membrane. It is difficult to separate it from the retina without causing harm to the retina. Therefore, visualization of the ILM with vital dyes was recommended.

The use of vital dyes to improve the visualization of intraocular tissues during vitrectomy has become a standard technique during vitrectomy. Recently this technique was named chromovitrectomy. (Rodrigues, Meyer et al. 2005)

### 1.3.2.1 Different dyes

To improve the precision of ILM-peeling and to avoid incomplete removal, different vital dyes have been introduced.

#### 1.3.2.1.1 Indocyanine green

The application of the indocyanine green (ICG) was firstly introduced in vitrectomy. ICG is a tricyanocyanine dye ( $C_{43}H_{47}N_2NaO_6S_2$ , 775 daltons) and contains 3% to 5% iodine. It has good affinity to the ILM and induces a cleavage plane that facilitates removal of the ILM. (Farah, Maia et al. 2009)

ICG-assisted vitrectomy was associated with high rates of macular hole closure in several series. However, there are reports on untoward effects of ICG in terms of visual outcome and peripheral visual field defects, and the dye is no more recommended in macular surgery.

#### 1.3.2.1.2 Trypan blue and membrane blue

Trypan blue (TB)/membrane blue (MB) is a dye from anterior segment surgery which is used in vitrectomy now. It is an anionic hydrophilic azo dye ( $C_{34}H_{24}N_6Na_4O_{14}S_4$ , 960daltons). Trypan blue has less affinity to the ILM compared with ICG, but it can stain cellular proliferations on the ILM sufficiently. (Farah, Maia et al. 2009) .

#### 1.3.2.1.3 Brilliant blue

Brilliant blue (BB) is a blue anionic aminotriarylmethane compound ( $C_{47}H_{48}N_3S_2O_7Na$ , 854 daltons). It's used in chromovitrectomy because of its selectively remarkable affinity for the ILM. It has been reported relatively safe because less toxic effect in animal research and

no toxic effect have been found in humans so far. (Farah, Maia et al. 2009)

## 2 MATERIALS AND METHODS

### 2.1 Laboratory Equipment

(1) +4 °C refrigerator  
(BOSCH, Germany)



(2) Incubator  
(Mettmert, Schwabach, Germany)



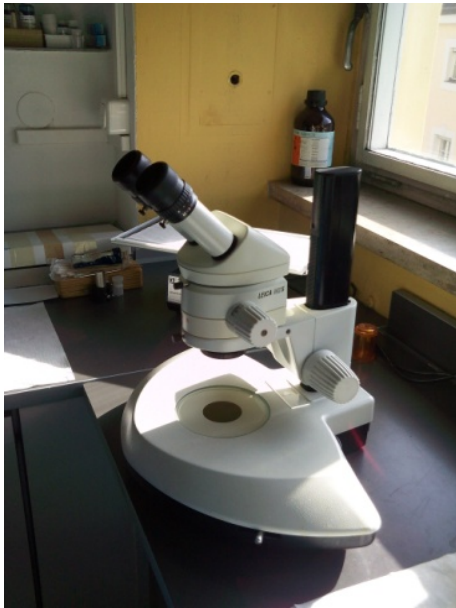
(3) Electronic balance Scout Pro SPU 202  
(Ohaus, Pine Brook, NJ USA)



(4) Shaker IKA-VIBRAX-VXR  
(IKA, Staufen, Germany)



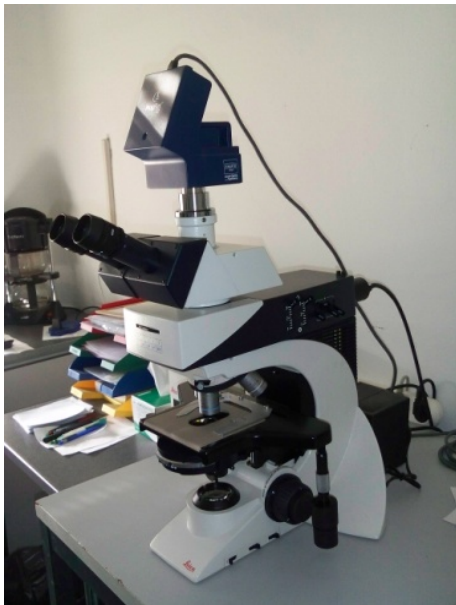
(5) Stereomicroscope Leica MS5  
(Leica, Germany)



(6) Captair®chem Filtair  
(erlab)



(7) Light microscope Leica DM2500  
(Leica, Wetzlar, Germany)



(8) Electron microscope Zeiss EM 9 S-2  
(Zeiss, Jena, Germany)



(9) Ultramicrotome Leica Ultracut R  
(Leica, Wien)



## 2.2 Reagents

Aqua dest (Braun 6724092)

$\text{Na}_2\text{B}_4\text{O}_7$  (Borax, MERCK 6306)

1%  $\text{CaCl}_2$  (Pharmacy of Ludwig-Maxmilians University, C08)

DDSA (SERVA 20755)

DMP 30 (SERVA 36975)

Epon 812 (SERVA 21045)

Ethanol (MERCK 1.00983)

25% Glutaraldehyde (Fluka 49626)

$\text{K}_2\text{Cr}_2\text{O}_7$  (Pharmacy of Ludwig-Maxmilians University)

Lead citrate (Fluka 15334)

MNA (SERVA 29452)

3.4%  $\text{NaCl}$  (Pharmacy of Ludwig-Maxmilians University, N18)

$\text{Na}_2\text{HPO}_4$  (MERCK 1.06346)

$\text{NaH}_2\text{PO}_4$  (MERCK 1.06580)

Osmium (Chempur 006051)

PBS Buffer (Pharmacy of Ludwig-Maxmilians University, G09)

1, 2-Propylenoxid (MERCK 1.12492)

Sodium citrate (Sigma S-4641)

1% Toluidine blue (Merck 115930)

Uranyl acetate (TED PELLA INC. 19481)

## 2.3 Prescription

1) 0.1M PBS (phosphate buffered saline)

$\text{Na}_2\text{HPO}_4 \cdot 2 \text{H}_2\text{O}$  14.42 g

- |    |   |                 |
|----|---|-----------------|
|    | NaH <sub>2</sub> PO <sub>4</sub> -H <sub>2</sub> O            | 2.62 g          |
|    | Distilled water to  | 1.0 l           |
|    | Adjust PH to 7.4 with HCl                                     |                 |
| 2) | 4% Glutaraldehyde   |                 |
|    | 25% Glutaraldehyde  | 16 ml           |
|    | 0.1M PBS to   | 100 ml          |
| 3) | 2% Osmium   |                 |
|    | Osmium  | 1 g             |
|    | Aqua dest   | 50 ml           |
|    | Then place in the +4 °C refrigerator overnight                |                 |
| 4) | 4% K <sub>2</sub> Cr <sub>2</sub> O <sub>7</sub> -KOH-bufffer |                 |
|    | K <sub>2</sub> Cr <sub>2</sub> O <sub>7</sub>                 | 4 g             |
|    | Aqua dest   | 80 ml           |
|    | Adjust PH to 7.4 with KOH 5N                                  |                 |
|    | Aqua dest   | 100 ml          |
| 5) | Dalton's fixative   |                 |
|    | 2% Osmium   | 20 ml           |
|    | 4% K <sub>2</sub> Cr <sub>2</sub> O <sub>7</sub> -KOH-bufffer | 10 ml           |
|    | 3.4% NaCl   | 4 ml            |
|    | 1% CaCl <sub>2</sub>  | 4 ml            |
|    | Aqua dest   | 2 ml            |
| 6) | Epon  |                 |
|    | Solution A  | Epon 812 62 ml  |
|    |   | a) DDSA 100 ml  |
|    | Solution B  | Epon 812 100 ml |
|    |   | b) MNA 89 ml    |
|    | Solution A and B can be stored at -20 °C                      |                 |
|    | Before use, mix solution A and solution B with DMP 30:        |                 |
|    | Solution A  | 9 ml            |
|    | Solution B  | 21 ml           |
|    | DMP 30  | 0.6 ml          |
| 7) | Mixture Propylenoxid+Epon                                     |                 |
|    | 1.2-Propylenoxid  | 20 ml           |
|    | Epon  | 20 ml           |
|    | Place at the room temperature overnight                       |                 |
| 8) | lead citrate  |                 |
|    | Lead citrate  | 1.33 g          |

---

Sodium citrate	1.76 g
Aqua dest.	30 ml

stark shake for ca. 30 min  
add 8 ml 1 M NaOH slowly till the solution is clear  
add Aqua dest to 50 ml  
Then place in refrigerator overnight, sealed and prevent from light.

## 2.4 Materials

From a consecutive series of surgical ILM-specimens removed at the University Eye Hospital Munich between 1998 and 2008, 109 specimens were randomly chosen from preexisting semithin sections. Six of 103 patients underwent surgery on both eyes. We included 79 eyes with macular holes and 30 eyes with other traction maculopathies which comprised of 17 specimens from eyes with macular pucker, 4 specimens from eyes with diabetic tractional oedema, 3 specimens from eyes with proliferative vitreoretinopathy and 6 specimens from eyes with vitreomacular traction syndrome. The surgical procedure was a standard three-port pars plana vitrectomy with peeling of the ILM and epiretinal tissue. Removal of the ILM was performed by experienced surgeons with and without intravitreal dye administration. Specimens without the ILM were excluded. Approval from the Institutional Review Board was obtained as well as the Informed Consent from each patient.

The patients' records were reviewed for age, gender, previous ocular surgery and preoperative history such as trauma. Additional information such as final best-corrected visual acuity, preoperative and postoperative status of the lens, and the period of follow-up examination was evaluated in those cases when cellular elements were seen at the retinal side of the ILM.

The surgical procedure enclosed the induction of a posterior vitreous detachment, if necessary, by suction with the vitrectomy probe over the optic nerve head. Removal of the ILM was performed by grasping the ILM with an end-gripping forceps and peeling it off the macular area. No dye was administered to visualize the ILM in 74 cases, meanwhile in 35 cases vital dye was administered. Trypan blue (Membrane blue, DORC, Netherlands) was used in 27 patients, brilliant blue (Brilliant peel, Geuder, Germany) was administered in 8 surgeries. Both dyes were administered in the fluid filled globe at a volume of 0.1 to 0.2 ml and washed out immediately. In case of coexisting cataract, a combined procedure was performed. In eyes with macular holes, the vitreous cavity was filled with a mixture of 15% C2F6, and the patients were recommended to stay in face-down position for up to five days.



## 2.5 Methods



Figure 2- 1

## 2.5.1 Preparation

The design of the project was to investigate all specimens with light microscopy. When large cellular fragments were found, electron microscopy was then performed. Therefore all specimens were processed by series sectioning for light microscopy. If cellular debris was present on the retinal side of the ILM, ultrathin sections were cut for transmission electron microscopy.

The preparation may be divided into eight steps: primary fixation, washing, postfixation, dehydration, infiltration with transitional solvents, infiltration with resin, embedding, and curing. (Figure 2-1)

### 2.5.1.1 Fixation

The purpose of fixation is to preserve the structure of living tissue, theoretically with no alteration from the living state. Additionally, fixation should protect tissues against disruption during embedding and sectioning and exposure to the electron beam.

Since all specimens were suitable for electron microscopy, glutaraldehyde was used as the fixative for all specimens, although formaldehyde penetrates tissue more readily than glutaraldehyde.

Glutaraldehyde's attribute as a fixative is in its ability to cross-link protein by virtue of the terminal aldehyde groups that make the molecule bifunctional. Specifically, the aldehyde groups react with  $\epsilon$ -amino groups of lysine in adjacent proteins, thereby cross-linking them.

The rate of penetration of glutaraldehyde into tissues is very slow. It can be expected to penetrate at a rate of less than 1 mm per hour if compact tissue is immersed into the glutaraldehyde. Therefore, the tissue should be under 1 mm in thickness at least in one dimension. This was the case in our series.

The specimens harvested during vitrectomy were immediately placed in phosphate-buffered 4% glutaraldehyde solution. The fixation lasted at least 2 hours at +8°C. After fixation the specimens were washed in 0.1 M phosphate-buffer at PH 7.4 for 10-15 minutes.

### 2.5.1.2 Washing

Aldehydes remaining from the primary fixation will be oxidized by osmium. Therefore, washing is important. It can eliminate free unreacted glutaraldehyde that remains within the tissues. The tissue is usually washed in the same buffer vehicle used for glutaraldehyde.

Unreacted glutaraldehyde will diffuse as slowly outward from the tissue as inward so that a minimum of a few hours of washing with changing buffer is recommended.

Each specimen was washed 2 times and it took 10 minutes for each time.

### 2.5.1.3 Postfixation

Standard glutaraldehyde-osmium tetroxide protocol was developed in 1963. Primary fixation with glutaraldehyde was followed by secondary exposure to osmium tetroxide.

Osmium tetroxide works as a secondary fixative of tissue by reacting primary with lipid moieties. It is widely believed that the unsaturated bonds of fatty acids are oxidized by osmium tetroxide. This reduced heavy metal adds density and contrast to the biological tissue. The molecular weight of osmium tetroxide is sufficiently high to be effective in scattering electrons.

The specimens were postfixated with Dalton's fixative for 2 hours.

### 2.5.1.4 Washing

After postfixation, the specimens were again washed with 0.1 M phosphate buffer 2 times. It took 10 minutes for each time.

### 2.5.1.5 Dehydration

Dehydration is the process of replacing the water in cells with a fluid that acts as a solvent between the aqueous environment of the cell and the hydrophobic embedding media. Ethanol is a common dehydrating agent. The specimens were dehydrated in graded concentrations of ethanol (30-50-70-90 and 100%) 2 times. Each time lasted 10 minutes.

### 2.5.1.6 Transitional solvent

Replacement of the dehydration solution by another intermediary solvent that is highly miscible with the plastic embedding medium is usually necessary to interface with the embedding media. The standard solvent used is propylene oxid, a highly volatile and a potentially carcinogenic liquid. It will also further dehydrate the tissue.

The specimens were placed in propylene oxid for 10-20 minutes. Then the specimens were placed in a mixture of propylene oxid and Epon at room temperature overnight.

### 2.5.1.7 Embedding

All specimens were embedded in Epon. Epon is the brand name of Epoxy embedding

media, which was introduced as an embedding medium by Glauert and subsequently modified by Luft. The hardness of the Epon mixture is controlled by the relative amount of DDSA (Dodecenylsuccinic anhydride) and NMA (Methyl Nadic anhydride), the former producing softer blocks and the latter harder blocker. The solution must be thoroughly mixed in a disposable plastic beaker using a resin mixer, a glass rod. The process can be accelerated by DMP (2, 4, 6-Tris (dimethylaminomethyl) phenol). The accelerator is added and mixed with the above.

The final step in embedding is curing the tissue blocks. With epoxy resins, a chain of polymerized resin is formed that crosslinks to other chains of resins to form an intergrated meshwork that totally permeates the tissue. Increased temperature accelerates the rate of hardening. Then the mixture was placed at +60 °C for 24-48 hours to polymerize.

## 2.5.2 Microtomy and Light microscopy

Light microscopy was performed in all 109 specimens. Series semithin sections of 1000 µm were cut by ultramicrotome Leica Ultracut R (Leica, Wien). The section was placed on a glass slide and stained with an aqueous mixture of 1% toluidine blue and 2% sodium borax. Overall, 1379 sections of 109 specimens were evaluated by light microscopy (mean value 12.7 sections per specimen).

Tissue sections were analyzed using a Leica light microscope (Leica, Wetzlar, Germany). The morphologic features of both the vitreal and the retinal side of the ILM were evaluated in terms of cell distribution, number of cells, and collagen distribution.

## 2.5.3 Electron microscopy

If cellular debris was present on the retinal side of the ILM, specimens were prepared for transmission electron microscopy. Ultrathin sections of 60-70nm were cut by ultramicrotome Leica Ultracut R (Leica, Wien). A Diamond Knife was used for ultramicrotomy. The sections were floated in distilled water and captured by a copper grid. From each specimen, serial sections of five grids with nine ultrathin sections were obtained. The ultrathin sections were contrasted with uranyl acetate for 15 minutes and with lead citrate for 10 minutes at room temperature.

A Zeiss EM 9 S-2 electron microscope was used for electron microscopy. Type and location of the cells, their relationship to the ILM, status of intracytoplasmic organelles such as nucleus, intracellular filaments and intracellular vesicles were documented.

The cellular elements on the retinal side of the ILM were quantified according to four groups as follows:

- 1) small (<1 µm in diameter) and solitarily distributed round cell fragments,
- 2) medium sized (1-2 µm in diameter) and accumulated round cell fragments,
- 3) large cell fragments (>2 µm in diameter),

- 4) complete cell bodies with cellular organelles.

## 2.5.4 Statistical Analysis

Statistical analysis of data was performed using the computer software (Statistical Package for the Social Science (SPSS) version 16.0).

Spearman rank correlation coefficient test, Pearson Chi- square test and Fisher's exact test were performed to evaluate the relationship between the presence of cell fragments on the retinal side and on the vitreal side, the relationship between the group with and without dye administration, and the relationship between macular hole and other retinopathies.

## 3 RESULTS

### 3.1 Clinical features

Forty-three right eyes and 66 left eyes were included in this series, corresponding to 76 woman and 33 men. Six patients underwent surgery on both eyes. The average age at time of surgery was 63.7 years (range 10 to 84 years). (Table 3 - 1) The age distribution of patients was as follows: <50 years (n=12), 50-60 years (n=17), 61-70 years (n=46), 71-80 years (n=30), >80 years (n=4). (Table 3 - 1)

The patients were divided into two groups: without vital dye and with vital dye administration. Each group contained two kinds of retinal diseases: macular hole and at least one kind of other maculopathies which included macular pucker, diabetic retinopathy, proliferative retinopathy and vitreomacular traction syndrome. In detail, we included 3 eyes with stage II macular holes, 24 eyes with stage III macular holes, 5 eyes with stage IV macular holes, 13 eyes with recurrent macular holes, 8 eyes with secondary macular holes (due to trauma or associated with retinal detachment), 6 eyes with primary macular pucker, 5 eyes with secondary macular pucker (after previous vitrectomy for retinal detachment), 1 eye with diffuse macular edema in proliferative diabetic retinopathy, 3 eyes with proliferative vitreoretinopathy and 6 eyes with vitreomacular traction syndrome in the group without dye administration; and in the group with dye administration, we included 2 eyes with stage II macular holes, 9 eyes with stage III macular holes, 6 eyes with stage IV macular holes, 6 eyes with recurrent macular holes, 3 eyes with secondary macular holes (due to trauma or associated with retinal detachment), 4 eyes with primary macular pucker, 2 eyes with secondary macular pucker (after previous vitrectomy for retinal detachment) and 3 eyes with proliferative diabetic retinopathy. (Table 3 - 2)

Only two types of vital dyes were selected in this study: membrane blue and brilliant blue. In 35 specimens with dye administration, we included 27 specimens with membrane blue and 8 specimens with brilliant blue. (Table 3 - 2)

## 3.2 Morphological features

### 3.2.1 Light microscopic features

1379 slices of 109 specimens were evaluated by light microscopy (mean value 12.7 slices per specimen).

Light microscopic examination showed the ILM as a continuous strand in all 109 specimens in low magnification (Figure 3 - 1). In higher magnification, two sides of the ILM could be distinguished by their different morphological characteristics: the retinal side of the ILM was undulated, and the vitreal side of the ILM was smooth (Figure 3 - 2). Cell debris or complete cells were observed on both sides of the ILM. In both groups of specimens, and in all five retinal diseases, cellular elements could be found on both sides of the ILM. Collagen was observed only on the vitreal side of the ILM. The morphologic features of both the vitreal and the retinal side of the ILM were evaluated in terms of cell distribution, number of cells, and collagen distribution. (Table 3 - 3, Table 3 - 4)

#### 3.2.1.1 Vitreal side of the ILM

On the vitreal side of the ILM, cells or cell fragment could be found directly attached to the ILM, or with collagen between cells and ILM.

Cells on the vitreal side of the ILM were arranged in a single-, mono- or multilayer. In this study, fibrocellular proliferation on the vitreal side of the ILM was seen in 41 specimens in the group without dye administration and in 20 specimens in the group of dye administration. In the group without dye administration, 32 specimens showed single cells and 9 cases presented with a mono- or multilayered cellular proliferation (Table 3 - 3), meanwhile in the dye administration group, 15 specimens showed single cells and 5 specimens presented with a mono- or multilayered cellular proliferation on the vitreal side of the ILM. (Table 3 - 4)

Collagen which was found on the vitreal side of the ILM was located between the ILM and cells. There are two distribution types of the collagen on the vitreal side of the ILM: focally present or present in a continuous strand. (Figure 3 - 3) In the group without dye administration, 10 specimens presented focal collagen and 2 specimens presented continuous collagen. (Table 3 - 3) In the dye administration group 9 specimens presented with focal collagen and 1 specimen presented continuous collagen. (Table 3 - 4)

In 32 specimens in the group without dye administration and in 15 specimens in the dye administration group, cells and collagen were absent.

### 3.2.1.2 Retinal side of the ILM

Complete retinal cells and large retinal cell fragments were found in 16 specimens at the ILM by light microscopy in the group without dye administration, which composed of 8 specimens from macular hole, 4 specimens from macular pucker, 1 specimen from diabetic maculopathy, 1 specimen from proliferative vitreomacular retinopathy and 2 specimens from vitreomacular traction syndrome. (Table 3 - 3) In the dye administration group 9 specimens were found on the retinal side of the ILM by light microscopy, which composed of 6 specimens from macular hole, 2 specimens from macular pucker and 1 specimen from diabetic maculopathy. (Table 3 - 4)

The retinal cell elements presented with single cells only. (Figure 3 – 5, Figure 3 – 6) No mono- or multilayer was found on the retinal side of the ILM.

Besides complete cells or large cell fragments, small cell fragments were also found on the retinal side of the ILM. No collagen was present on the retinal side of the ILM.

### 3.2.1.3 Single cells crossing the ILM

In 109 specimens, three cells in 2 specimens were found crossing the ILM. One specimen with 2 cells crossing the ILM was from a patient with recurrent macular hole without dye administration. (Figure 3 – 7) Another case that showed a single cell crossing the ILM was from patient with stage IV macular hole with brilliant blue administration.



## 3.2.2 Electron microscopic features

### 3.2.2.1 ILM in electron microscopy

Ultrastructural evaluation focused on the 25 specimens that showed cells or cellular debris on the retinal side of the ILM. In each specimen that was found with retinal cellular elements at the ILM, the presence of retinal cell fragments or retinal cell bodies could be confirmed in ultrathin sections. (Figure 3 - 8)

### 3.2.2.2 Four distinct morphologic patterns of retinal structures

Four distinct morphologic patterns were observed on the retinal side of the ILM that were quantified as follows:

- (1) Small (<1  $\mu\text{m}$  in diameter) round cell fragments were solitarily distributed and mostly directly adjacent to the ILM. The cell fragments resembled plasma membrane remnants of Müller cell endfeet, and they often appeared disrupted and electron-dense with direct contact to the undulations of the ILM. (Figure 3-9)
- (2) Medium sized (1-2  $\mu\text{m}$  in diameter) round cell fragments were found with and without contact to the ILM. Their electron density was variable. Therefore, the cell fragments appeared to originate from different structures such as Müller cell endfeet, optic nerve fibers, or ganglion cell remnants. (Figure 3-10)
- (3) Large cell fragments of more than 2  $\mu\text{m}$  in diameter were frequently found surrounded by smaller cell fragments with multiple remnants of plasma membranes. They appeared to originate from Müller cell endfeet and Müller cell processes as well as from optic nerve fiber bundles. (Figure 3-11)
- (4) Entire retinal cell bodies with cellular organelles such as nucleus, mitochondria, intracytoplasmic vesicles and filaments were seen in direct contact to the ILM. (Figure 3-12)

### 3.2.2.3 Pattern of cellular elements depending on the disease in the group without dye administration

In the group without dye administration, specimens from eyes with macular holes showed retinal cell debris mainly of medium or large size, whereas specimens from eyes with other traction maculopathies mostly presented with large cell fragments or complete retinal cells. (Table 3 - 8)

In specimens removed from macular holes eyes, retinal cell fragments were mostly

smaller than those from eyes with other traction maculopathies. Large retinal cell bodies were seen in 63% of all eyes with macular holes. Large retinal cell bodies and complete retinal cell were seen in 88% of eyes with other traction maculopathies. Complete retinal cell bodies were not seen in eyes with macular holes, but in 63% of eyes with other traction maculopathies.

### 3.2.3 Comparison between different groups

#### 3.2.3.1 Cell proliferation

To investigate whether the retinal damage was correlated with the vitreal cellular proliferation, the presence of cell debris on both sides of the ILM was evaluated.

In all 109 specimens, cells or cell fragments were found in 61 specimens on the vitreal side and in 25 specimens on the retinal side of the ILM. Among the 25 specimens that showed retinal cells at the ILM, 18 specimens (72.0%) showed vitreal cells at the same time. In contrast, among the 61 specimens that presented without vitreal cell fragments, retinal debris were seen in 18 (29.5 %) specimens. (Table 3 - 5)

Spearman rank correlation coefficient test/Pearson Chi- square test was performed to evaluate whether the presence of cell fragments on the retinal side was related to the presence of cell proliferation on the vitreal side. No significant correlation was seen between the presence of retinal cells and vitreal cells. (Spearman rank correlation coefficient test  $P = 0.067$ , Pearson Chi- square test  $P = 0.066$ )

#### 3.2.3.2 Dye administration

To investigate whether the cellular presence on the retinal side of the ILM was correlated with dye administration, the retinal cell debris in patients with idiopathic macular holes and idiopathic macular pucker in the group with and without dye administration was evaluated.

In the group without dye administration, retinal cells were found in 5 specimens (13.2%) and were not found in 33 specimens. In the group with dye administration, retinal cells were found in 8 specimens (38.1%) and were not found in 13 specimens. A significant difference was seen between the presence of retinal debris between the two groups. (Pearson Chi-square test  $P = 0.027$ ) (Table 3 - 6)

#### 3.2.3.3 Diseases

To investigate whether the presence of retinal cell fragments depended on the underlying disease, specimens of macular hole patients and specimens with other maculopathies were evaluated.

In the group without dye administration, retinal cell fragments were found in 8 specimens (15.1%) of macular holes and 8 specimens (38.1%) of other maculopathies. There was significantly less retinal cell debris in macular holes than in other traction maculopathies such as macular pucker, vitreomacular traction syndrome, diabetic retinopathy, and proliferative vitreoretinopathy (Pearson Chi-square test  $P=0.030$ ). (Table 3 - 7)

In the group with dye administration, retinal cell fragments were found in 6 specimens of macular holes and in 3 specimens with other maculopathies. No significant difference was seen between macular holes and other traction maculopathies. (Fisher's exact test  $P=0.665$ )

## Figures and tables

Figure 3 - 1 ILM in low magnification

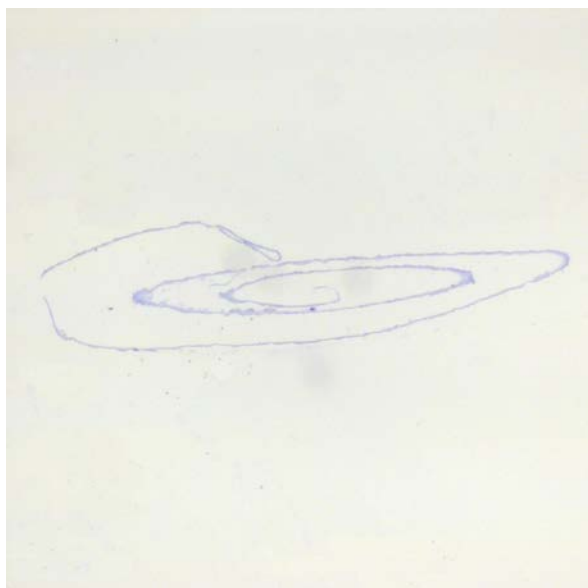


Figure 3- 1: Light microscopy of semithin section showing an entire specimen. The ILM was stained blue with a mixture of 1% toluidine blue and 2% sodium borax. (Original magnification: 10x)

Figure 3 - 2 ILM in high magnification

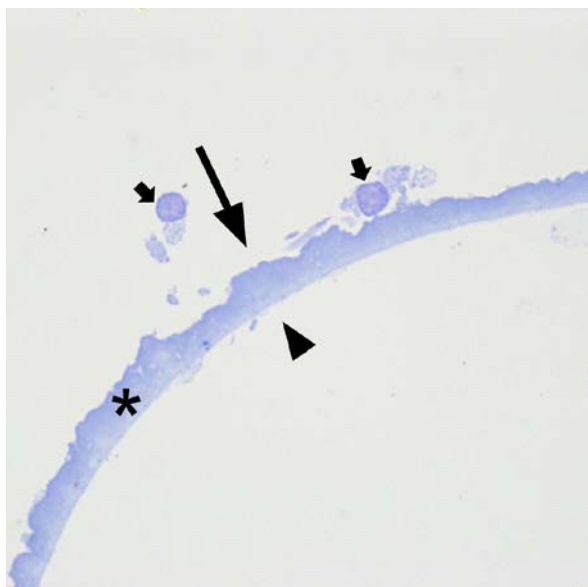


Figure 3- 2: Light microscopy of ILM stained with a mixture of 1% toluidine blue and 2% sodium borax. The ILM (asterisk) was showing a smooth vitreal side (arrowhead) and an undulating retinal side (long arrow). Two cells with a complete cell nucleus (short arrow) were present on the retinal side of the ILM. (Original magnification: 100x)

Figure 3 - 3 Singel cell on the vitreal side

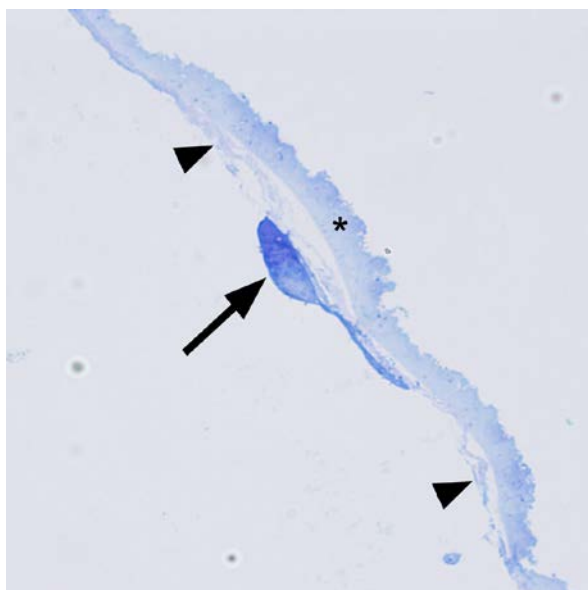


Figure 3- 3: Light microscopy of the ILM stained with the mixture of 1% toluidine blue and 2% sodium borax. A single cell (arrow), which was present on the vitreal side of the ILM, was separated from the ILM (asterisk) by a continuous strand of collagen fibers (arrowhead). (original magnification: 100x)

Figure 3 - 4 Mono-/multilayer on the vitreal side

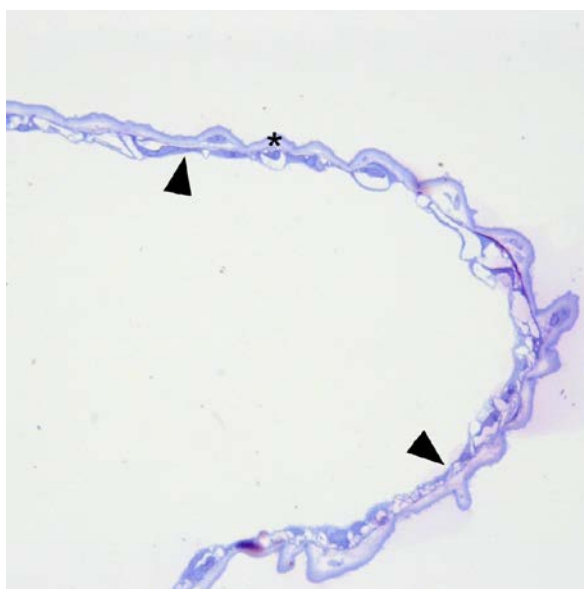


Figure 3- 4: Light microscopy of the ILM stained with the mixture of 1% toluidine blue and 2% sodium borax. A mono-/multilayer (arrowhead) was present on the vitreal side of the ILM (asterisk). (Original magnification: 40x)

Figure 3 - 5 Singel cell on the retinal side

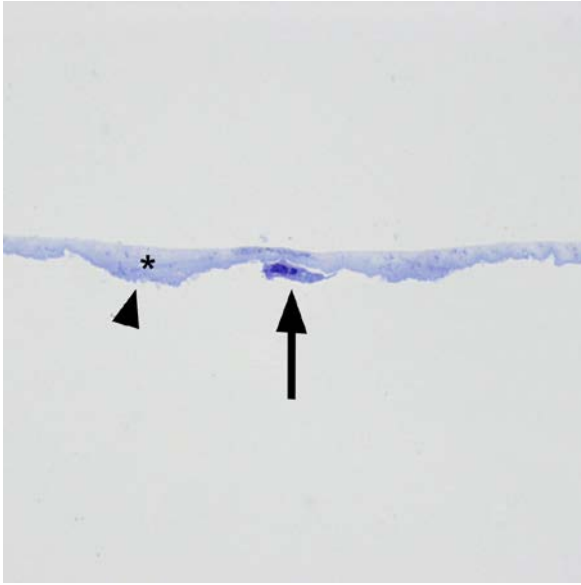


Figure 3- 5: Light microscopy of the ILM from a patient with stage IV macular hole. A single cell (arrow) was present on the retinal side (arrowhead) of the ILM (asterisk). (Original magnification: 100x)

Figure 3 - 6 Cells on the retinal side

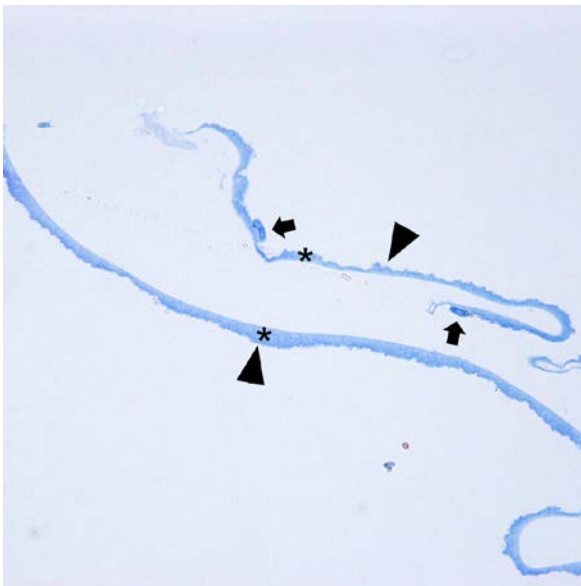


Figure 3-6: Light microscopy of the ILM from patient with proliferative vitreoretinopathy. Two single cells (short arrow) were present on the retinal side (arrowhead) of the ILM (asterisk). (Original magnification: 40x)

Figure 3 - 7 Cell crossing the ILM

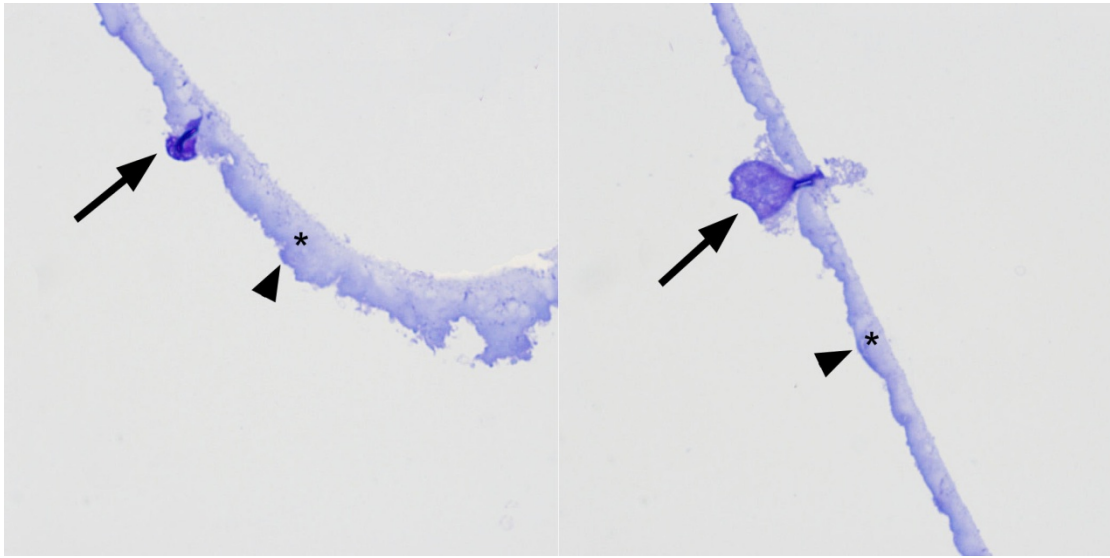


Figure 3-7: Light microscopy of the ILM from patient with persistent macular hole. A cell (arrow) on the retinal side (arrowhead) crossing the ILM (asterisk). (Original magnification: 100x)

Figure 3 - 8 The presence of retinal cell fragments in light- and electronmicroscopy

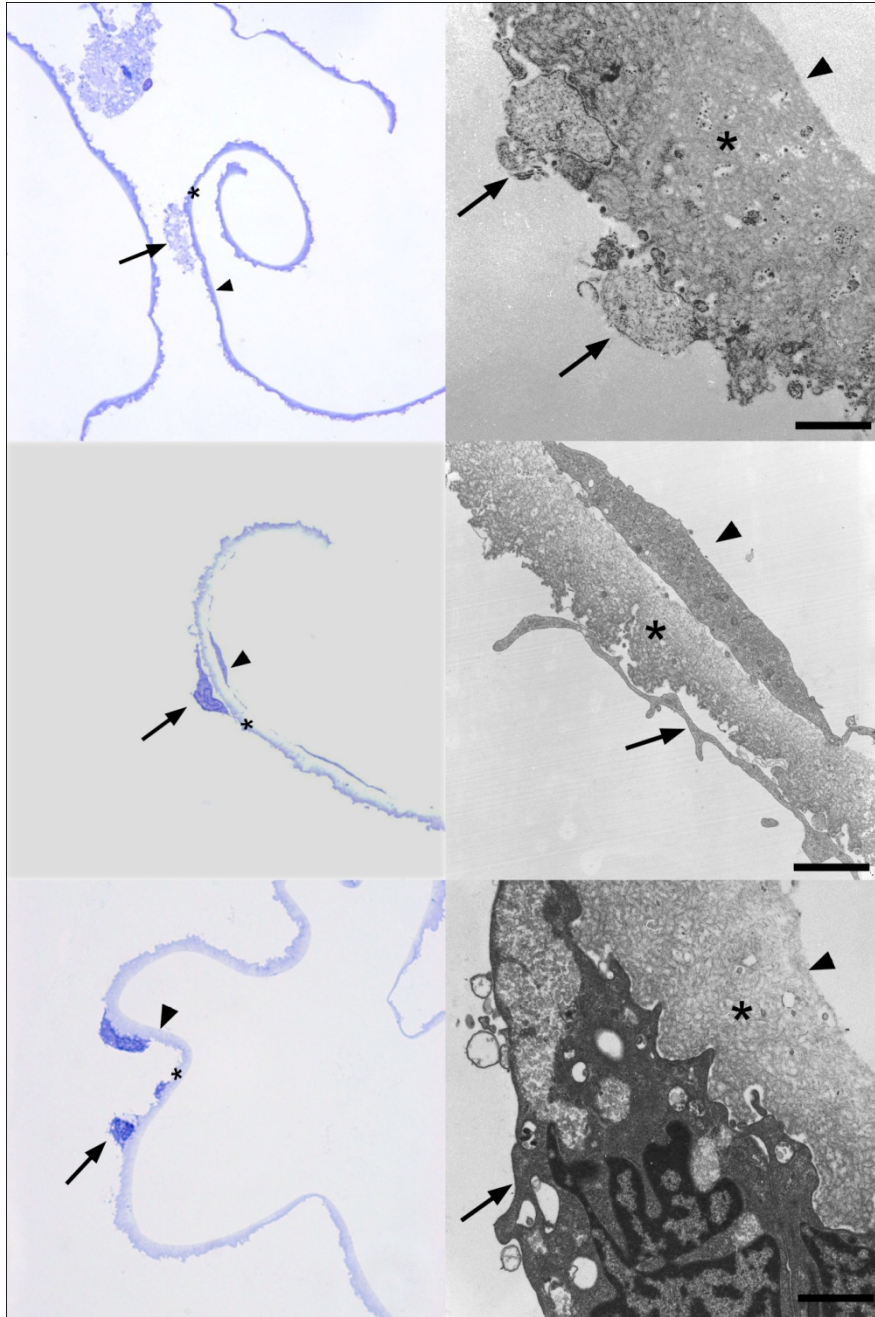


Figure 3-8: Left, light micrographs (LM) and, right, transmission electron micrographs (TEM) of the internal limiting membrane (ILM) (asterisk) removed from eyes with diabetic macular edema, stage IV idiopathic macular hole, and proliferative vitreoretinopathy (from top to bottom). The ILM is characterized by an undulated retinal side and a smooth vitreal side.

(Top) Plasma membrane fragments (arrow) on the retinal side of the ILM. The vitreal side of the



---

ILM (arrowhead) is devoid of cells and collagen. (specimen removed for diabetic macular edema, original magnification: LM 40x; TEM x9500, bar=1.0  $\mu$ m)

(Middle) LM shows a cell with nucleus on the retinal side of the ILM, EM shows one large cell fragment (arrow) in contact with ILM (asterisk), and a single cell on the vitreal side of the ILM (arrowhead) which shares features with fibrous astrocytes such as masses of intermediate type filaments, rough endoplasmic reticulum and electrondense particles. (specimen removed for stage IV idiopathic macular hole, original magnification: LM 100x; TEM x4800, bar=2.0  $\mu$ m)

(Bottom) Entire cell body with cellular nucleus (arrow) located on the retinal side of the ILM (asterisk). The vitreal side of the ILM (arrowhead) is blank. (specimen removed for proliferative vitreoretinopathy, original magnification: LM 100x; TEM x9500, bar=1.0  $\mu$ m)

Figure 3 - 9 Morphologic pattern 1

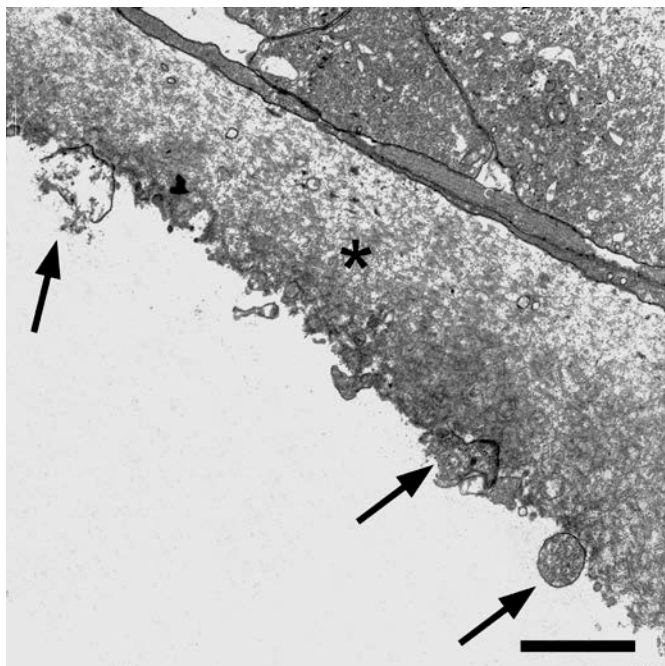


Figure 3- 9: Electron microscopy of the ILM (asterisk) from a patient with persistent macular hole showing small ( $< 1 \mu\text{m}$  in diameter) and solitarily distributed round cell fragments (arrow) on the retinal side of the ILM. (original magnification:  $\times 9500$ , bar= $1.0 \mu\text{m}$ )

Figure 3 - 10 Morphologic pattern 2

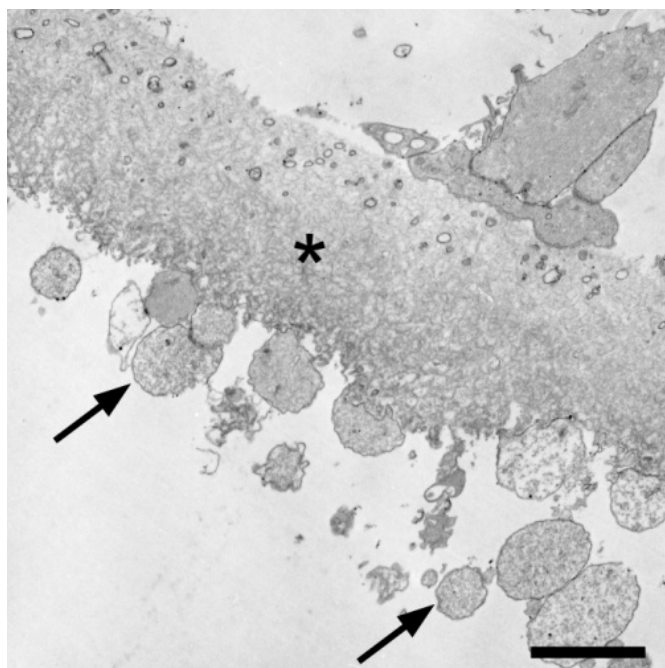


Figure 3- 10: Electron microscopy of the ILM (asterisk) from a patient with persistent macular hole showing medium sized (1-2  $\mu\text{m}$  in diameter) round cell fragments (arrow) (original magnification: x4800, bar=2.0  $\mu\text{m}$ )

Figure 3 - 11 Morphologic pattern 3

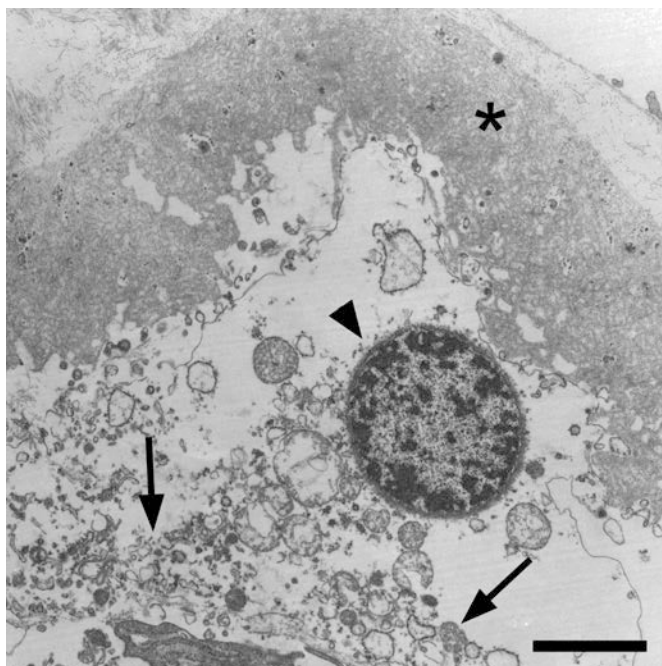


Figure 3- 11: Electron microscopy of the ILM (asterisk) from patient with vitreomacular traction syndrome showing a ruptured cell with a cell nucleus (arrowhead) and multiple remnants of plasma membranes (arrow). The nucleus is round and regular, contoured with fine granules of chromatin. It is approximately 3  $\mu\text{m}$  in diameter. (original magnification: x4800, bar=2.0  $\mu\text{m}$ )

Figure 3 - 12 Morphologic pattern 4

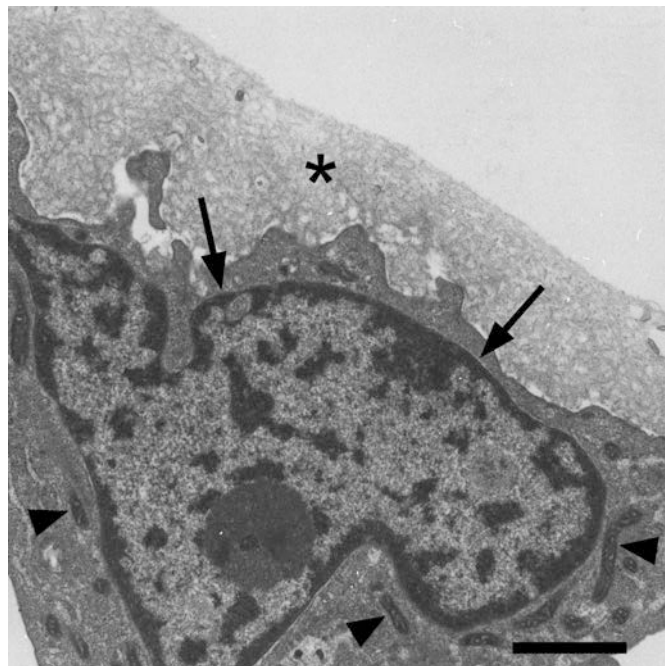


Figure 3- 12: Electron microscopy of the ILM (asterisk) from a patient with proliferative vitreoretinopathy showing a complete cell with cell nucleus (arrow) with approximately 10  $\mu\text{m}$  in diameter on the retinal side of the ILM. The irregular contoured, undulated nucleus was presenting with nucleoli and chromatin mostly distributed along the caryomembrane. Its plasma membrane fills the undulations of the ILM and the cytoplasm is found with abundant mitochondria (arrowhead), endoplasmatic reticulum and golgi complexes.

Table 3 - 1 Clinical Features

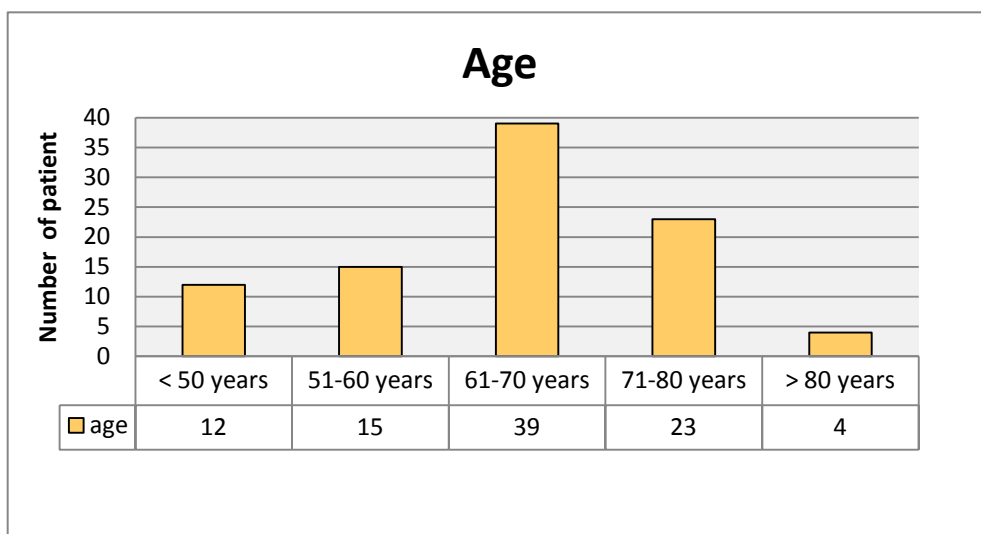
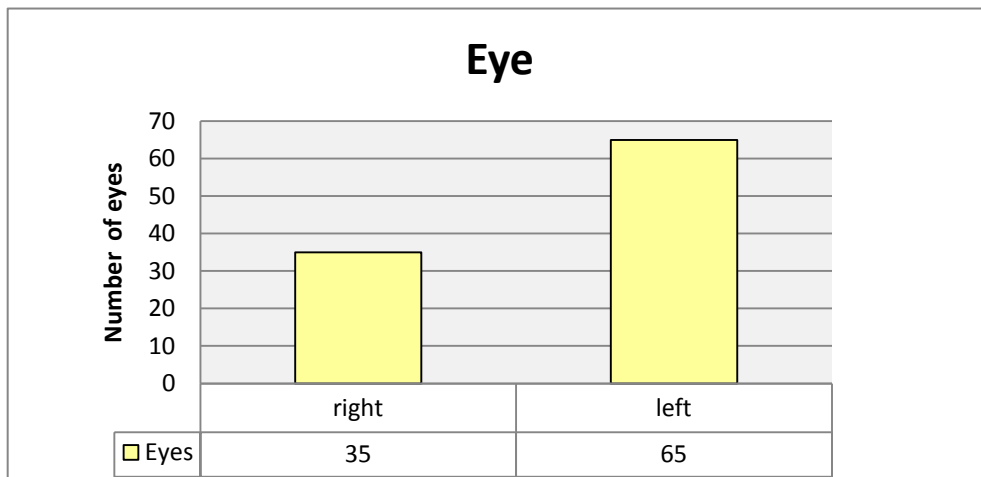
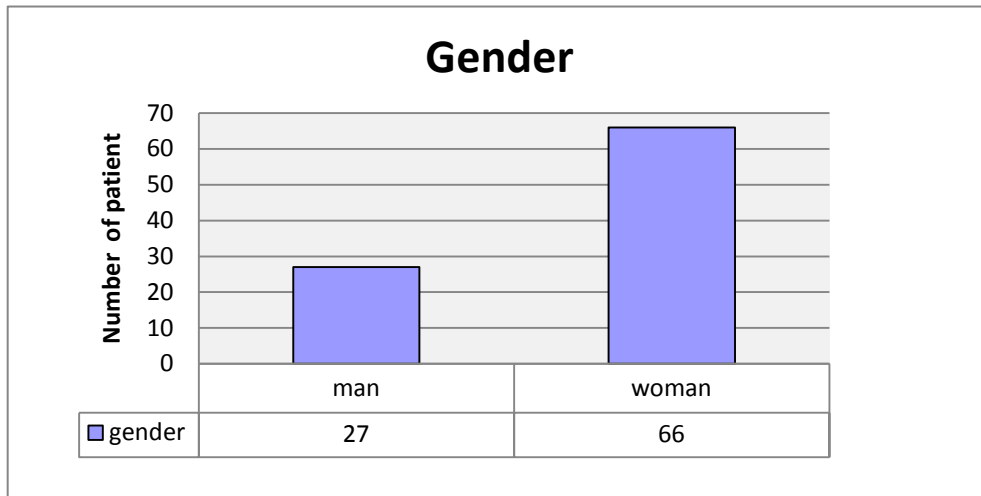


Table 3 - 2 Number of the specimens

Diagnose		Without dye administration	With dye administration		total
			BB	MB	
Macular holes	stage II	3	2		5
	stage III	24		9	33
	stage IV	5	3	3	11
	recurrent	13		6	19
	secondary	8		3	11
macular pucker	primary	6	3	1	10
	secondary	5		2	7
proliferative diabetic retinopathy		1		3	4
proliferative vitreoretinopathy		3			3
vitreomacular traction syndrome		6			6
<b>total</b>		<b>74</b>	<b>35</b>		<b>109</b>

Table 3 - 3 Evaluation of specimens without dye administration by light microscopy

Diagnosis		number of specimens		Cells on vitreal side of the ILM			Vitreous collagen	Cells on retinal side of the ILM		
				single cell	Mono/multilayer	total		single cell	total	
macular holes	macular hole stage II	3	53	0	0	0	25	0	0	8
	macular hole stage III	24		11	2	13		2	2	
	macular hole stage IV	5		2	1	3		1	2	
	Recurrent macular hole	13		5	3	8		1	3	
	Secondary macular hole	8		1	0	1		1	1	
macular pucker	Primary macular pucker	6	11	4	0	4	16	2	1	4
	Secondary macular pucker	5		4	0	3		1	3	
Diabetic retinopathy		1	1	1	0	1	0	1	1	8
Proliferative vitreoretinopathy		3	3	2	0	2	1	1	1	
Vitreomacular traction syndrome		6	6	2	3	6	3	2	2	
total		74		32	9	41	12	16		



Table 3 - 4 Evaluation of specimens with dye administration by light microscopy

Diagnosis		number of specimens		Cells on vitreal side of the ILM				Vitreal collagen	Cells on retinal side of the ILM		
				single cell	Mono/multilayer	total			single cell	total	
macular holes	macular hole stage II	2		0	1	1	15	0	2	6	
	macular hole stage III	9		3	1	4		3	1		
	macular hole stage IV	6		2	1	3		2	3		
	Recurrent macular hole	6		3	2	5		3	0		
	Secondary macular hole	3		2	0	2		1	0		
macular pucker	Primary macular pucker	4		2	0	2	5	1	2	2	3
	Secondary macular pucker	2		1	0	1		0	0		
Diabetic retinopathy		3		2	0	2		0	1	1	
Proliferative vitreoretinopathy		/		/	/	/		/	/		
Vitreomacular traction syndrome		/		/	/	/		/	/		
<b>total</b>		<b>35</b>		<b>15</b>	<b>5</b>	<b>20</b>	<b>10</b>	<b>9</b>			

Table 3 - 5 Presence of cellular elements on the retinal and vitreal side of the ILM in all specimens

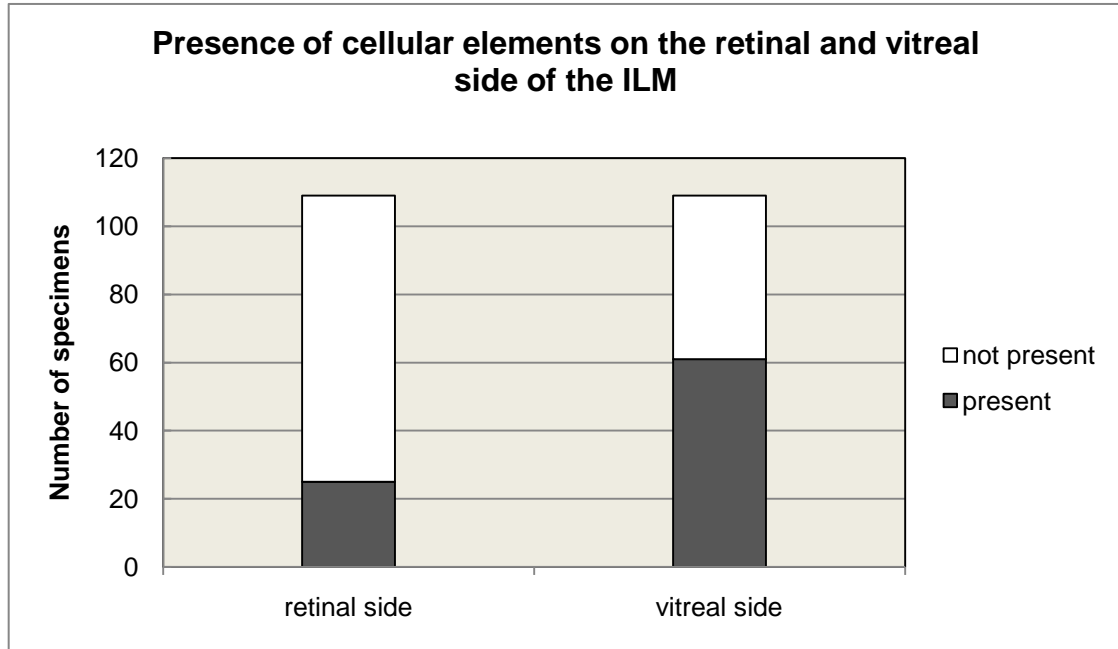


Table 3 - 6 Presence of retinal cell elements in patients with idiopathic macular holes and macular pucker

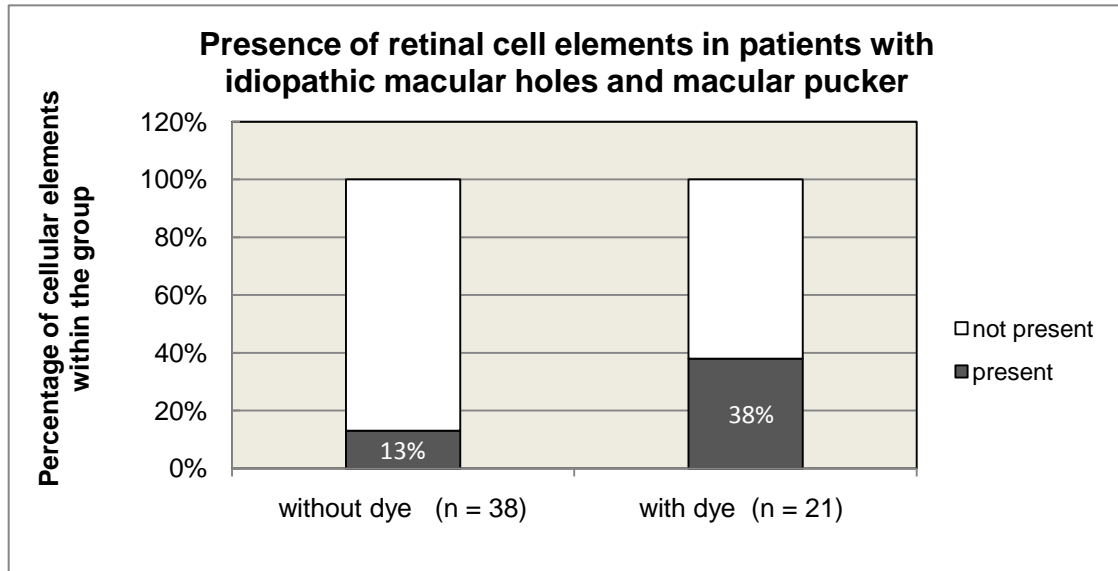


Table 3 - 7 Presence of retinal cell elements depending on the disease in the group without dye administration

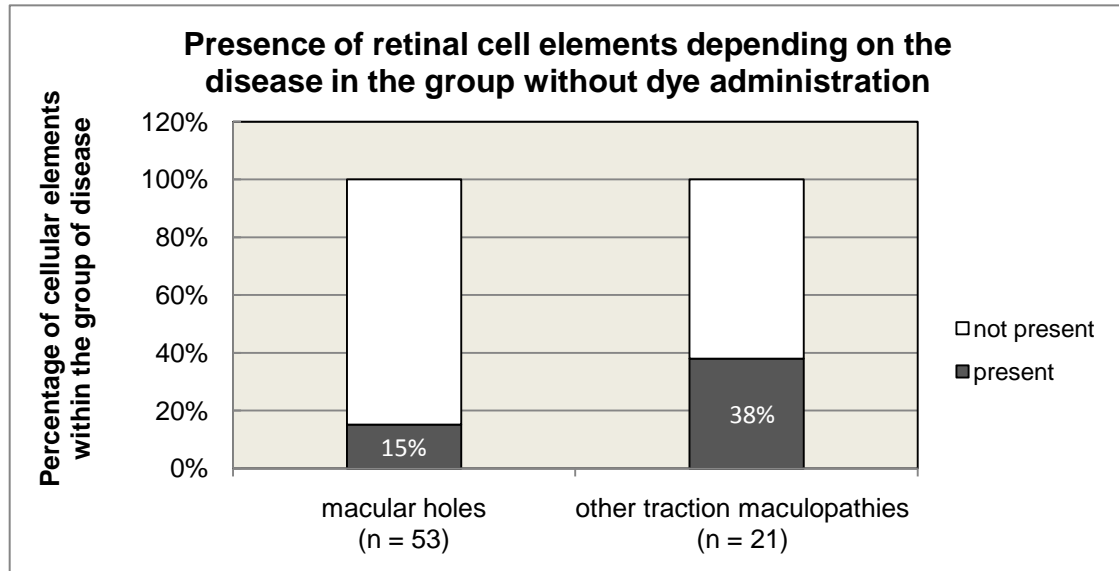


Table 3 - 8 Four patterns of cellular elements on the retinal side of the ILM in the group without dye administration

Patterns of cellular elements	Macular holes			Other traction maculopathies			
	idiopathic	reccurent	secondary	MP	DR	PVR	VMTS
small	1						
medium	1	1		1			
large	2	2	1	2			
complete cell				1	1	1	2
Total number (%) of the case	4/32 (12.5%)	3/13 (23.1%)	1/8 (12.5%)	4/11 (36.4%)	1/1 (100%)	1/3 (33.3%)	2/6 (33.3%)

MP: macular pucker

DR: diabetic retinopathy

PVR: proliferative vitreoretinopathy

VMTS: vitreomacular traction syndrome

## 4 DISCUSSION

### 4.1 Principal findings

#### 4.1.1 Morphologic changes on both sides of the ILM

The ILM plays a role as a structural boundary between the vitreous and the retina. It has a smooth vitreal surface and an irregular retinal surface, due to its close apposition with the plasma membrane of the Müller cell endfeet.

Given the close anatomic relationship, removal of the ILM may damage inner retinal layers. The structural evidence of retinal cell fragments in surgical ILM specimens can be interpreted as an indicator for retinal changes induced by vitreoretinal surgery, especially by peeling of the ILM.

In the present study, retinal fragments of ILM removed by vitreoretinal surgery were observed in 16 specimens without vital dye administration and in 9 specimens with dye administration. In these 109 specimens, we included macular hole patients, and other maculopathies such as macular pucker, diabetic retinopathy, proliferative vitreoretinopathy and vitreomacular traction syndrome. The retinal damage was evaluated in three aspects: cell fragments on both sides of the ILM were observed to evaluate if the retinal damage was related to the vitreal cell proliferation, i.e. to the underlying disease; cell fragments in patients with idiopathic macular holes and idiopathic macular pucker were investigated in the group with and without dye administration (birilliant blue and membrane blue), in order to evaluate if the retinal changes were related to the administration of vital dyes.

The answers to the questions were:

1. Cell fragments were found in 25 specimens on the retinal side of the ILM and in 61 specimens on the vitreal side of the ILM by light microscopy. No significant correlation was seen between the presence of retinal cells and vitreal cells;
2. When comparing eyes with idiopathic macular holes and macular pucker, retinal cells were found in 5 specimens (13.2%) in the group without dye administration, and in 8 specimens (38.1%) in the group with dye administration. There was a significant difference between the two groups.
3. In the group without dye administration, retinal cell fragments were found in 8 specimens (15.1%) of macular holes and 8 specimens (38.1%) of other maculopathies. There was significantly less retinal cell debris in macular holes than in other traction maculopathies such as macular pucker, diabetic retinopathy, proliferative vitreoretinopathy and vitreomacular traction syndrome; in the group with dye administration, retinal cell fragments were found in 6 specimens of macular holes and in 3 specimens of other maculopathies. No significant difference was seen between macular holes and other traction maculopathies when dye was used.

Concerning the potential origin of retinal cells and cell fragments at the ILM, small cell debris found on the retinal side of the ILM in the present study as well as in previous investigations may correspond to fragments of retinal structures attached to the ILM such as Müller cell endfeet, or disrupted nerve fiber.

In accordance with previous work of our group, small fragments of the Müller cell plasma membrane were found on the retinal side of the ILM in all specimens. Entire cell bodies of retinal cells were primarily found in patients with other traction maculopathies than macular holes, and in patients with additional dye application.

#### 4.1.2 Explaining of the results

In this study, we collected two groups of specimens, those without vital dye administration and those with Membrane Blue/Brilliant Blue administration. To avoid the influence of other confounding factors, we compared the presence of retinal cells between the two groups only in idiopathic macular holes and idiopathic macular pucker specimens. Significant less retinal cell fragments were seen in the group without dye administration.

We included five diseases in the group without dye administration: macular holes, macular pucker, diabetic retinopathy, proliferative vitreoretinopathy and vitreomacular traction syndrome. The results in this study showed significantly less retinal cell debris in macular holes than in the other traction maculopathies. Previous research suggested that both vitreous traction and cellular proliferation play an essential role in the pathogenesis of all these five disease. For macular holes, tangential vitreoretinal traction is the initial cause of macular hole development, cell migration and cell proliferation on both sides of the ILM appear to be a secondary event. (Schumann, Schaumberger et al. 2006) For the other four diseases, cell proliferation and epiretinal membrane formation are primary changes resulting in epimacular cellular proliferation. (Gandorfer, Messmer et al. 2000; Gandorfer, Rohleder et al. 2002; Gandorfer, Rohleder et al. 2005)

To qualify retinal cells or cell fragments, four morphological patterns were chosen with respect to different size of the retinal debris. Specimens from eyes with macular holes showed retinal cell debris mainly of medium or large size, whereas specimens from eyes with other traction maculopathies mostly presented with large cell fragments or complete retinal cells.

#### 4.2 Strengths and weaknesses of the study

This is the first study on retinal elements adherent to the ILM following surgery in a large series. The study provides the morphological changes on both sides of the ILM after surgery in 5 diseases with and without dye assistance.

The study's main limitation is due to the conventional preparation procedure for electron microscopic analysis. Only cross sections of ILM specimens were observed that were

obtained by series sectioning. However, there is no more accurate evaluation of cell proliferation at the ILM than transmission electron microscopy. Recently, a new preparation procedure for light microscopy and interference microscopy proposed flat mounted ILM specimens for cell quantification, but a differentiation between the vitreal side and the retinal side of the ILM would not have been possible with this technique. (Gandorfer, Scheler et al. 2009)

The relatively small number of other traction maculopathies compared with the number of macular holes is another limitation of this study, because the cases of other maculopathies are not so frequent as cases of macular holes.

### 4.3 Strengths and weaknesses in relation to other studies

By light microscopy of series sections, 109 ILM specimens were screened. Retinal cell debris were found in 25 cases. By transmission electron microscopy, these 25 ILM specimens mostly showed large retinal cell fragments of more than 2  $\mu\text{m}$  in diameter as well as entire retinal cells. The presence of retinal cell remnants at the ILM appeared to depend on the underlying disease when no dye applied. Large cell fragments and complete retinal cells were seen more often in traction maculopathies other than macular holes. In macular holes, 15.1% of the ILM specimens without dye administration were found with cellular remnants on the retinal side of the ILM. This is consistent with results of a study on the ultrastructure of stage III and IV idiopathic macular holes removed without dye assistance when 12 (13%) of 92 cases were seen with retinal cell debris. (Schumann, Schaumberger et al. 2006) However, the latter study only found small cell fragments whereas this study showed large cell fragments and complete retinal cells in 63% of all macular holes including idiopathic macular holes as well as recurrent macular holes.

The herein demonstrated small and medium sized round retinal cell fragments were identified as plasma membrane of Müller cells and fragments of Müller cell endfeet. Similar structures have already been reported in other studies. Haritoglou reported round structures on the retinal side of the ILM in patients with macular holes after conventional peeling of the ILM during the surgery. These round structures are supposed to represent inner portions of the Müller cells torn away with the ILM. In comparison with undulated areas of the retinal side of ILM, only very tiny cellular fragments can be seen in areas where the retinal surface of the ILM appears smooth. (Haritoglou, Schumann et al. 2006) Tari reported a similar structure with transport vesicles in it and indicated that the structures were Müller cell end feet. (Tari, Vidne-Hay et al. 2007)

Several studies assumed that retinal cell remnants at the ILM originate from Müller cell footplates which directly insert at the characteristic undulations of the retinal side of the ILM. (Sebag 1992; Smiddy, Feuer et al. 2001; Wolf, Schnurbusch et al. 2004; Schumann, Schaumberger et al. 2006)

Large retinal cell fragments and complete retinal cells in ILM specimens removed without dye assistance appear to originate not exclusively from Müller cells. Some ultrastructural characteristics of these cells such as round and regular nuclei, fine granules of



chromatin may be attributed to astrocytes and occasionally to oligodendroglia. (Villegas 1964) Whole retinal cells with electron-dense nuclei found at the ILM may present cells of still unknown origin. A similar phenotype of cells has recently been found following a multilayered glial cell proliferation underneath the ILM in eyes with macular pucker. (Haritoglou, Schumann et al. 2007)

#### 4.4 Meaning of the study

The exact mechanisms of the pathogenesis of cellular proliferation on both sides of the ILM are still unclear. Given the close anatomic relationship, removal of the ILM may change the architecture of inner retinal layers. The structural evidence of retinal cell fragments in surgical ILM specimens can be interpreted as an indicator for retinal changes induced by vitreoretinal surgery. Since large cellular remnants on the retinal side of the ILM were seen after ILM removal with intravitreal administration of ICG (Gandorfer, Haritoglou et al. 2001; Haritoglou, Gandorfer et al. 2002; Schumann, Schaumberger et al. 2006; Schumann, Gandorfer et al. 2009), this study was primarily conducted to evaluate the presence of large retinal cell fragments in ILM specimens removed without dye assistance.

Müller cells are thought to play a key role in the maintenance of retinal homeostasis and function. (Newman and Reichenbach 1996; Newman 2004; Metea and Newman 2007) They significantly modulate neuronal activity by controlling the concentration of neuroactive substances. (Szatkowski, Barbour et al. 1990) Thus, the adherence of Müller cell fragments at the ILM during ILM removal might induce neurosensory retinal damage. This hypothesis is supported by reports on transient b-wave depressions in focal macular electroretinograms and visual field defects after ILM-peeling in macular hole surgery. (Haritoglou, Ehrt et al. 2001; Terasaki, Miyake et al. 2001)

By electron microscopy, Wolf and colleagues demonstrated structural damage of inner retinal layers following ILM peeling. (Wolf, Schnurbusch et al. 2004) In human donor retina, a substantial number of Müller cell endfeet and Müller cell processes were severely damaged even at the margins of the peeled area. However, these human donor eyes were peeled with ICG assistance. There is evidence that ILM peeling with intravitreal ICG administration in macular surgery may have worse functional outcomes caused by ICG related retinal toxicity. (Gandorfer, Haritoglou et al. 2001; Gandorfer, Haritoglou et al. 2003; Gass, Haritoglou et al. 2003; Haritoglou, Gandorfer et al. 2003; Ando, Sasano et al. 2004; Rodrigues, Meyer et al. 2007) The dye-related retinal toxicity may act as a multifactorial process that may include an alteration of the cleavage plane by changing the biomechanical features of the ILM. (Haritoglou, Gandorfer et al. 2002; Gandorfer, Haritoglou et al. 2003; Wollensak, Spoerl et al. 2004)

In the context of mechanical damage and dye-related toxicity, the present study could serve as a basis to compare the presence of retinal fragments after ILM peeling with administration of novel dyes.

## 4.5 Unanswered questions and future research

Although this study gave us some basement data to suggest the origin of cell proliferation on both sides of the ILM, the real origin of these cells is still not clear. Further studies and immunohistochemical investigations are needed to differentiate between the cells and clarify whether fragments of nerve fibers and retinal neurons could also be torn off by ILM removal.

## References

- Al-Abdulla, N. A., J. T. Thompson, et al. (2004). "Results of macular hole surgery with and without epiretinal dissection or internal limiting membrane removal." *Ophthalmology* **111**(1): 142-149.
- Ando, F., K. Sasano, et al. (2004). "Anatomic and visual outcomes after indocyanine green-assisted peeling of the retinal internal limiting membrane in idiopathic macular hole surgery." *Am J Ophthalmol* **137**(4): 609-614.
- Barber, A. J., D. A. Antonetti, et al. (2000). "Altered expression of retinal occludin and glial fibrillary acidic protein in experimental diabetes. The Penn State Retina Research Group." *Invest Ophthalmol Vis Sci* **41**(11): 3561-3568.
- Bloom, G. D. and E. A. Balazs (1965). "An electron microscopic study of hyalocytes." *Exp Eye Res* **4**(3): 249-255.
- Brooks, H. L., Jr. (2000). "Macular hole surgery with and without internal limiting membrane peeling." *Ophthalmology* **107**(10): 1939-1948; discussion 1948-1939.
- Bussow, H. (1980). "The astrocytes in the retina and optic nerve head of mammals: a special glia for the ganglion cell axons." *Cell Tissue Res* **206**(3): 367-378.
- Cooper, M. E., D. Vranes, et al. (1999). "Increased renal expression of vascular endothelial growth factor (VEGF) and its receptor VEGFR-2 in experimental diabetes." *Diabetes* **48**(11): 2229-2239.
- El-Labban, N. G. and K. W. Lee (1983). "Myofibroblasts in central giant cell granuloma of the jaws: an ultrastructural study." *Histopathology* **7**(6): 907-918.
- Eyden, B., S. S. Banerjee, et al. (2009). "The myofibroblast and its tumours." *J Clin Pathol* **62**(3): 236-249.
- Farah, M. E., M. Maia, et al. (2009). "Dyes in ocular surgery: principles for use in chromovitrectomy." *Am J Ophthalmol* **148**(3): 332-340.
- Fine, B. S. and A. J. Tousimis (1961). "The structure of the vitreous body and the suspensory ligaments of the lens." *Arch Ophthalmol* **65**: 95-110.
- Foos, R. Y. (1972). "Vitreoretinal juncture; topographical variations." *Invest Ophthalmol* **11**(10): 801-808.
- Gandorfer, A., C. Haritoglou, et al. (2001). "Indocyanine green-assisted peeling of the internal limiting membrane may cause retinal damage." *Am J Ophthalmol* **132**(3): 431-433.
- Gandorfer, A., C. Haritoglou, et al. (2003). "Retinal damage from indocyanine green in experimental macular surgery." *Invest Ophthalmol Vis Sci* **44**(1): 316-323.
- Gandorfer, A., E. M. Messmer, et al. (2000). "Resolution of diabetic macular edema after surgical removal of the posterior hyaloid and the inner limiting membrane." *Retina* **20**(2): 126-133.
- Gandorfer, A., M. Rohleder, et al. (2005). "Epiretinal pathology of diffuse diabetic macular edema associated with vitreomacular traction." *Am J Ophthalmol* **139**(4): 638-652.
- Gandorfer, A., M. Rohleder, et al. (2002). "Epiretinal pathology of vitreomacular traction syndrome." *Br J Ophthalmol* **86**(8): 902-909.
- Gandorfer, A., R. Scheler, et al. (2009). "Interference microscopy delineates cellular

- proliferations on flat mounted internal limiting membrane specimens." Br J Ophthalmol **93**(1): 120-122.
- Gass, C. A., C. Haritoglou, et al. (2003). "Functional outcome of macular hole surgery with and without indocyanine green-assisted peeling of the internal limiting membrane." Graefes Arch Clin Exp Ophthalmol **241**(9): 716-720.
- Gass, J. D. (1988). "Idiopathic senile macular hole. Its early stages and pathogenesis." Arch Ophthalmol **106**(5): 629-639.
- Gass, J. D. (1995). "Reappraisal of biomicroscopic classification of stages of development of a macular hole." Am J Ophthalmol **119**(6): 752-759.
- Gotzinger, E., M. Pircher, et al. (2008). "Retinal pigment epithelium segmentation by polarization sensitive optical coherence tomography." Opt Express **16**(21): 16410-16422.
- Guidry, C. (2005). "The role of Muller cells in fibrocontractive retinal disorders." Prog Retin Eye Res **24**(1): 75-86.
- Gupta, P., A. A. Sadun, et al. (2008). "Multifocal retinal contraction in macular pucker analyzed by combined optical coherence tomography/scanning laser ophthalmoscopy." Retina **28**(3): 447-452.
- Haritoglou, C., O. Ehrh, et al. (2001). "Paracentral scotomata: a new finding after vitrectomy for idiopathic macular hole." Br J Ophthalmol **85**(2): 231-233.
- Haritoglou, C., A. Gandorfer, et al. (2002). "Indocyanine green-assisted peeling of the internal limiting membrane in macular hole surgery affects visual outcome: a clinicopathologic correlation." Am J Ophthalmol **134**(6): 836-841.
- Haritoglou, C., A. Gandorfer, et al. (2003). "The effect of indocyanine-green on functional outcome of macular pucker surgery." Am J Ophthalmol **135**(3): 328-337.
- Haritoglou, C., C. A. Gass, et al. (2001). "Macular changes after peeling of the internal limiting membrane in macular hole surgery." Am J Ophthalmol **132**(3): 363-368.
- Haritoglou, C., R. Schumann, et al. (2006). "Evaluation of the internal limiting membrane after conventional peeling during macular hole surgery." Retina **26**(1): 21-24.
- Haritoglou, C., R. G. Schumann, et al. (2007). "Glial cell proliferation under the internal limiting membrane in a patient with cellophane maculopathy." Arch Ophthalmol **125**(9): 1301-1302.
- Heegaard, S. (1997). "Morphology of the vitreoretinal border region." Acta Ophthalmol Scand Suppl(222): 1-31.
- Kampik, A., K. R. Kenyon, et al. (1981). "Epiretinal and vitreous membranes. Comparative study of 56 cases." Arch Ophthalmol **99**(8): 1445-1454.
- Kelly, N. E. and R. T. Wendel (1991). "Vitreous surgery for idiopathic macular holes. Results of a pilot study." Arch Ophthalmol **109**(5): 654-659.
- Krieg, T., D. Abraham, et al. (2007). "Fibrosis in connective tissue disease: the role of the myofibroblast and fibroblast-epithelial cell interactions." Arthritis Res Ther **9 Suppl 2**: S4.
- Kwok, A., T. Y. Lai, et al. (2005). "Epiretinal membrane surgery with or without internal limiting membrane peeling." Clin Experiment Ophthalmol **33**(4): 379-385.
- la Cour, M. and J. Friis (2002). "Macular holes: classification, epidemiology, natural history and treatment." Acta Ophthalmol Scand **80**(6): 579-587.

- Lister, W. (1924). "Holes in the Retina and Their Clinical Significance." Br J Ophthalmol **8**(1): i4-20.
- McDonnell, P. J., S. L. Fine, et al. (1982). "Clinical features of idiopathic macular cysts and holes." Am J Ophthalmol **93**(6): 777-786.
- Mester, V. and F. Kuhn (2000). "Internal limiting membrane removal in the management of full-thickness macular holes." Am J Ophthalmol **129**(6): 769-777.
- Metea, M. R. and E. A. Newman (2007). "Signalling within the neurovascular unit in the mammalian retina." Exp Physiol **92**(4): 635-640.
- Newman, E. and A. Reichenbach (1996). "The Muller cell: a functional element of the retina." Trends Neurosci **19**(8): 307-312.
- Newman, E. A. (2004). "A dialogue between glia and neurons in the retina: modulation of neuronal excitability." Neuron Glia Biol **1**(3): 245-252.
- Park, D. W., P. U. Dugel, et al. (2003). "Macular pucker removal with and without internal limiting membrane peeling: pilot study." Ophthalmology **110**(1): 62-64.
- Park, D. W., J. O. Sipperley, et al. (1999). "Macular hole surgery with internal-limiting membrane peeling and intravitreal air." Ophthalmology **106**(7): 1392-1397; discussion 1397-1398.
- Pastor, J. C., E. R. de la Rúa, et al. (2002). "Proliferative vitreoretinopathy: risk factors and pathobiology." Prog Retin Eye Res **21**(1): 127-144.
- Patel, J. I., P. G. Hykin, et al. (2006). "Pars plana vitrectomy with and without peeling of the inner limiting membrane for diabetic macular edema." Retina **26**(1): 5-13.
- Rodrigues, E. B., C. H. Meyer, et al. (2005). "Chromovitrectomy: a new field in vitreoretinal surgery." Graefes Arch Clin Exp Ophthalmol **243**(4): 291-293.
- Rodrigues, E. B., C. H. Meyer, et al. (2007). "Mechanisms of intravitreal toxicity of indocyanine green dye: implications for chromovitrectomy." Retina **27**(7): 958-970.
- Ryter, A. (1985). "Relationship between ultrastructure and specific functions of macrophages." Comp Immunol Microbiol Infect Dis **8**(2): 119-133.
- Schumann, R. G., A. Gandorfer, et al. (2009). "VITAL DYES FOR MACULAR SURGERY: A Comparative Electron Microscopy Study of the Internal Limiting Membrane." Retina.
- Schumann, R. G., M. M. Schaumberger, et al. (2006). "Ultrastructure of the vitreomacular interface in full-thickness idiopathic macular holes: a consecutive analysis of 100 cases." Am J Ophthalmol **141**(6): 1112-1119.
- Scott, I. U., A. L. Moraczewski, et al. (2003). "Long-term anatomic and visual acuity outcomes after initial anatomic success with macular hole surgery." Am J Ophthalmol **135**(5): 633-640.
- Scott, J. E. (1992). "The chemical morphology of the vitreous." Eye **6 ( Pt 6)**: 553-555.
- Sebag, J. (1991). "Age-related differences in the human vitreoretinal interface." Arch Ophthalmol **109**(7): 966-971.
- Sebag, J. (1992). "Anatomy and pathology of the vitreo-retinal interface." Eye **6 ( Pt 6)**: 541-552.
- Sebag, J. and G. S. Hageman (2000). "Interfaces." Eur J Ophthalmol **10**(1): 1-3.
- Smiddy, W. E., W. Feuer, et al. (2001). "Internal limiting membrane peeling in macular hole surgery." Ophthalmology **108**(8): 1471-1476; discussion 1477-1478.
- Smiddy, W. E., A. M. Maguire, et al. (1989). "Idiopathic epiretinal membranes. Ultrastructural

- characteristics and clinicopathologic correlation." *Ophthalmology* **96**(6): 811-820; discussion 821.
- Strauss, O. (2009). "[The role of retinal pigment epithelium in visual functions]." *Ophthalmologie* **106**(4): 299-304.
- Szatkowski, M., B. Barbour, et al. (1990). "Non-vesicular release of glutamate from glial cells by reversed electrogenic glutamate uptake." *Nature* **348**(6300): 443-446.
- Tari, S. R., O. Vidne-Hay, et al. (2007). "Functional and structural measurements for the assessment of internal limiting membrane peeling in idiopathic macular pucker." *Retina* **27**(5): 567-572.
- Terasaki, H., Y. Miyake, et al. (2001). "Focal macular ERGs in eyes after removal of macular ILM during macular hole surgery." *Invest Ophthalmol Vis Sci* **42**(1): 229-234.
- van Furth, R., J. A. Raeburn, et al. (1979). "Characteristics of human mononuclear phagocytes." *Blood* **54**(2): 485-500.
- Villegas, G. M. (1964). "Ultrastructure of the Human Retina." *J Anat* **98**: 501-513.
- Walshe, R., P. Esser, et al. (1992). "Proliferative retinal diseases: myofibroblasts cause chronic vitreoretinal traction." *Br J Ophthalmol* **76**(9): 550-552.
- Watanabe, T. and M. C. Raff (1988). "Retinal astrocytes are immigrants from the optic nerve." *Nature* **332**(6167): 834-837.
- Wolf, S., U. Schnurbusch, et al. (2004). "Peeling of the basal membrane in the human retina: ultrastructural effects." *Ophthalmology* **111**(2): 238-243.
- Wollensak, G., E. Spoerl, et al. (2004). "Influence of indocyanine green staining on the biomechanical strength of porcine internal limiting membrane." *Ophthalmologica* **218**(4): 278-282.

## Acknowledgements

I take the opportunity to thank Professor Dr. Anselm Kampik for the friendly scientific environment in the Eye Hospital of the Ludwig-Maximilians University of Munich. I am also grateful for his suggestion in project design and for the support in providing specimens in this project.

I would like to express my sincere thanks to my supervisor, Professor Dr. Arnd Gandorfer, who lead me in this research field and gave me valuable professional advice. He always supported me with his unlimited encouragement and understanding. His enthusiasm and diligence in his work is going to be a lifelong example in my scientific career.

I would like to give my sincere thanks to Dr. Ricarda Schumann for the uncountable advices and friendly cooperation. She taught me how to accomplish a scientific work. From the collecting of data to the paper writing, she guided me warmly in each step of this project.

I would also like to thank Mrs. Renate Scheler, the kind colleague in the lab, who taught me the laboratory techniques, and was always ready to give me help when I had problems.

As well I extend my gratitude to PD Dr. Haritoglou and PD Dr. Grüterich for providing specimens, to Dr. Markus Schaumberger for the helps in statistic, and to all colleagues who gave me the help to complete this project.

And finally, I would like to thank all members of my family, my parents, my grandma, and my husband for the selfless love, patience and waiting. The support of my family always was the assurance and motivation during my medical studies.

# Curriculum Vitae

## Name

Yang Yang

## Date of Birth

27. Mar. 1979

## Place of Birth

Wuhan, Hubei Province, P.R.China

## Citizenship

Chinese

## Address in China

Miaodun Street 48, Zi.2-502, Wuhan 430030, P.R.China

## Present address

Knorrstr.29, Zi.306, 80807 Munich, Germany

## Marital status

Married

## Education

Sep.1985-Jun.1991: Primary school

Yuemachang Primary school, Wuhan

Sep.1991-Jun.1994: Junior high school

Shouyi Junior high school

Sep.1994-Jun.1997: High school

No.1 Middle School Attached to Central China Normal University

Sep.1997-Jun.2003: Bachelor of Medicine

Tongji Medical College of Huazhong University of Science & Technology (HUST)

Sep.2003-Jun.2006: Master in Science (Ophthalmology)

Tongji Medical College of Huazhong University of Science & Technology (HUST)

From Sep.2006: Promotion

Eye Hospital of the Ludwig-Maximilians University of Munich